NACA RM E50G11

NACA

RESEARCH MEMORANDUM

INVESTIGATION OF EFFECTS OF INLET-AIR VELOCITY DISTORTION ON PERFORMANCE OF TURBOJET ENGINE

By E. William Conrad and Adam E. Sobolewski

Lewis Flight Propulsion Laboratory
Cleveland, Ohio

NATIONAL ADVISORY COMMITTEE FOR AERONAUTICS

WASHINGTON

September 13, 1950

NATIONAL ADVISORY COMMITTEE FOR AERONAUTICS

RESEARCH MEMORANDUM

INVESTIGATION OF EFFECTS OF INLET-AIR VELOCITY DISTORTION ON PERFORMANCE OF TURBOJET ENGINE

By E. William Conrad and Adam E. Sobolewski

SUMMARY

An investigation was conducted in the NACA Lewis altitude wind tunnel to determine the effect of nonuniform inlet-air velocities on the performance of a full-scale axial-flow turbojet engine. Total-pressure variations as large as 103 pounds per square foot in the radial direction and 90 pounds per square foot in the circumferential direction at 30,000-foot altitude were obtained by the use of obstructions in the engine-inlet ducting. Data were obtained at altitudes from 20,000 to 50,000 feet at a flight Mach number of approximately 0.21 and corrected engine speeds from 77.3 percent of rated speed to rated engine speed.

For some of the configurations and operating conditions investigated, the effect of distortions of the inlet-velocity pattern on the internal aerodynamics of the engine resulted in slight improvements in performance; at other operating conditions the performance was slightly impaired. These effects are distinct from the performance losses associated with losses in ram-pressure recovery. With the inlet-velocity distortions investigated, the net thrust varied between 0.95 and 1.03 of the net thrust with the uniform inlet configuration at the same operating conditions. Similarly, the ratio of specific-fuel-consumption values varied from 1.00 to 1.04. In general, compressor efficiencies were slightly reduced by the nonuniform inlet-velocity distributions. It may therefore be concluded that performance changes due to the effects of nonuniform inlet velocity on the internal aerodynamics of the engine investigated do not appear to be serious for the range of distortions investigated.

Throughout the investigation, engine-vibration measurements were carefully observed. Vibration readings were always well below the limits specified by the manufacturer.

INTRODUCTION

Flight installations of turbojet engines vary greatly in the manner in which air is supplied to the engine. If an engine is submerged in the fuselage or the wing, the airplane designer usually must compromise the ducting design to avoid interference with the pilot's compartment, structural members, or auxiliary equipment. The degree of compromise in the internal aerodynamics of the airplane (inlet ducting and exhaust pipe) as compared with the external aerodynamics or the location of auxiliary equipment should be based on a knowledge of the relative sacrifices incurred in performance and serviceability. Performance changes incurred by compromising the inlet-duct design may be attributed to losses in ram-pressure recovery and to the effects of nonuniform air velocity at the compressor inlet. The magnitude of performance losses resulting from poor ram-pressure recovery is given in reference 1. Data are presented herein to show the effect of nonuniform engine-inlet air velocity on the over-all engine and component performance.

Data were obtained on a full-scale axial-flow turbojet engine for a range of flight conditions and corrected engine speeds from 77.3 percent of rated engine speed to rated engine speed. Six configurations formed by changing the inlet-duct geometry and installing obstructions in the inlet duct were used to obtain velocity gradients in both the radial and circumferential directions. Radial total-pressure variations up to 103 pounds per square foot and circumferential variations up to 90 pounds per square foot at an altitude of 30,000 feet were obtained. The inlet-velocity distribution is shown for each configuration; the tendency of the distortions to persist through the engine and the effects on performance are discussed.

APPARATUS AND PROCEDURE

Engines

Two engines of similar type were used for this investigation. Principal components of the engines were an axial-flow multistage compressor, direct-flow combustors, and a single-stage turbine. The first rotor stage of the compressor had a hub-to-tip diameter ratio of 0.65. At zero-ram, sea-level conditions and rated engine speed, the compressor Mach number was 0.894. A variable-area exhaust nozzle was used to obtain a range of engine (and compressor) pressure ratios at each engine speed and flight conditions.

Installation

The engine was mounted on a wing in the test section of the altitude wind tunnel. The six inlet configurations used in the investigation are shown in figure 1. Configurations A, B, and C (fig. 1(a)) were used with the first engine, and D, E, and F (fig. 1(b)) were used with the second engine. The first and second engines were of similar design except that the accessory housing in the engine-inlet duct was longer for the second engine and the standard engine-inlet screen was not installed.

A bellmouth entrance section used with configuration A (fig. 2(a)) was installed to obtain the engine performance with a uniform radial and circumferential velocity profile at the engine inlet, thereby providing a basis for comparison of the performance with configurations B and C. Configuration B conformed to the usual test installation in the altitude wind tunnel with the engine air supplied to the engine by means of the make-up air ram pipe. Configuration B was modified to form configuration C by the installation of a series of 1-inch spoilers in the ram pipe (fig. 2(b)). These spoilers were designed to increase the displacement thickness of the boundary layer on the outside wall.

Data were necessary for configuration D, which was similar to A, to serve as a standard of comparison for configurations E and F, inasmuch as the lack of engine-to-engine reproducibility would not permit a comparison of the performance of configurations E and F with that of A, which was investigated with the first engine. To form configuration E, an annular fine-mesh screen 4 inches high was installed around the spinner 8 inches ahead of the instrumentation at station 1 and 44 inches ahead of the compressor-inlet guide vanes. This screen was designed to reduce the air velocity near the spinner. The annular screen was removed and two screens in the form of 60° segments were installed across the annulus at the same axial location to form configuration F. These obstructions were formed by layers of screen so arranged that the solidity was greatest over the center 30° of each segment. The resulting uneven circumferential velocity distribution was intended to simulate the distribution that might occur in flight installations that incorporate twin-inlet ducts.

Instrumentation

Fixed instrumentation for measuring pressures and temperatures was installed at various stations in the engine (fig. 3). Details

of the instrumentation at the engine inlet and compressor inlet and outlet are given in figure 4. Only the instrumentation pertinent to this investigation is given in detail. For all configurations except E, air flow was calculated from pressure and temperature measurements at the engine inlet (station 1). Engine air flows for configuration E were determined by the engine performance characteristics according to the method described in the appendix.

Sperry-M.I.T. vibration pick-ups were mounted in both vertical and horizontal planes at the compressor outlet and turbine flanges. A filter was used in the vibration meter to prevent a response at vibrational frequencies below 60 cycles per second.

Simulated Flight Conditions

At each of the conditions listed in the following table, complete engine performance data were obtained at several engine pressure ratios by varying the exhaust-nozzle area:

Altitude (ft)	Corrected engine speed (percent of rated speed)	Configuration
20,000	77.3	E
25,000	100	A, C
25,000	91.3	A, B, C
25,000	78.5	A, B, C,
30,000	93.7	D, F
30,000	89.9	D, F
30,000	85.1	D, F
30,000	77.3	D, E, F
35,000	100	A, C
35,000	91.3	A, B, C
35,000	78.5	A, B, C
45,000	100	A, C
45,000	91.3	A, B
45,000	78.5	A, B
50,000	100	A, C
50,000	91.3	A, B, C,
50,000	78.5	A, B, C,

Data were obtained at only two flight conditions with configuration E due to a temporary limitation of tunnel facilities.

All data were taken at a nominal ram-pressure ratio of 1.03, which would correspond to a flight Mach number of 0.21 if no inlet ducting losses occurred. The ram-pressure ratio that was used in obtaining the experimental data was set by means of a single total-pressure probe at station 1 and a static-pressure probe in the tunnel test section. The actual ram-pressure ratio for all configurations, as determined from the average of all the total-pressure tubes at station 1, varied from 1.015 to 1.032; the effect of this variation on the engine pumping characteristics, however, is negligible. It is noted that inasmuch as velocity distortions represent energy losses, a much higher flight Mach number is required to produce a given average total pressure at the engine inlet when the ducting is such that the engine-inlet velocity is severely distorted.

Experimental Procedure

For configurations B and C, dry refrigerated air was supplied to the engine inlet through a duct from the tunnel make-up air system. The air flow through the duct (ram pipe) was throttled from approximately sea-level pressure to a total pressure at the engine inlet corresponding to the desired flight conditions. Pressures corresponding to the desired flight conditions were also obtained at the engine inlet with the other four configurations; however, the air was taken directly from the tunnel through a bellmouth entrance.

When the desired engine speed, altitude, and approximate ram-pressure ratio were obtained, automatic-recording, self-balancing potentiometers (flight recorders) were started. A complete cycle of the temperatures required took approximately 1 minute. During the flight recorder cycle, instantaneous readings of pressures and of engine instruments were obtained by photographing banks of manometers and the engine instrument panel. At the same time, the engine fuel flow was obtained from calibrated rotameters.

Analysis Procedure

For given values of ambient pressure, engine-inlet pressure, temperature ratio, and engine air flow, the complete performance of a turbojet engine can be determined from pumping-characteristic curves as explained in reference 2. A pumping-characteristic curve

at 30,000 feet for configuration D is shown in figure 5. Similar curves for the other configurations were determined but are not presented in this report. The comparative performance of the various configurations was determined from these curves at common values of engine total-temperature ratio and engine-inlet total pressure (average value downstream of obstructions, station 1).

The engine temperature ratios selected are as follows:

Corrected engine speed (percent of rated speed)	Engine temperature ratio T_5/T_1	Configurations compared
100.0	3.38	A, C
93.7	2.80	D, F
91.3	3.15	A, B, C
89.9	2.80	D, F
85.1	2.80	D, F
78.5	2.78	A, B, C
77.3	2.60	D, E, F

With the exception of the value for the lowest engine speed, the temperature ratios selected fall within the band of values obtained during previous performance investigations of the same type engine with fixed-area exhaust nozzles. The temperature ratio used for the lowest engine speed was slightly high because the data were insufficient to permit a comparison at temperature ratios corresponding to fixed-area-nozzle operation. Symbols and methods of calculation are given in the appendix.

RESULTS AND DISCUSSION

The pattern and the magnitude of the inlet flow distortions investigated are given by typical plots of a velocity-distribution parameter, which is defined as the ratio of the local velocity head to the average velocity head for the entire flow area q_l/q_{av}. The tendency of the flow irregularities to persist or to disappear in passing through the engine is discussed, and the effects of the distortions on the component and over-all engine performance are given.

Inlet-velocity distribution. - The data of figure 6 are typical of the data for all configurations in that changes of engine speed or altitude had no appreciable effect on the velocity distribution pattern at the engine inlet. The various inlet patterns obtained are therefore characteristic only of the geometry of the inlet ducting. The radial velocity distributions characteristic of configurations A to E are shown in figure 7. The radial patterns for different circumferential positions for configuration F were similar to that of D but of different magnitudes. Each data point shown in figure 7 represents the average value at a given radial position as obtained from total-pressure tubes at either three or four circumferential positions (fig. 4). A study of the data revealed that the average static pressure measured at the engine inlet (used in computing q_l and q_{av}) was sufficiently reliable for all configurations except configuration E where the screen was installed around the spinner. With configuration E, the severity of the distortion and the proximity of the obstruction to the instrumentation apparently resulted in radial static-pressure gradients too severe to be measured at station 1, with the result that the quantitative values of the curve may be somewhat in error. The general shape of the curve, however, is believed to be correct.

The installation of the bellmouth entrance section with no obstructions (configurations A and D, fig. 7) was intended to produce the uniform inlet velocity normally assumed in design calculations and was used as a basis of comparison for the other configurations. Over the extent covered by the instrumentation the velocity parameter varied only 0.09 for configuration A and 0.35 for configuration D.

Boundary-layer buildup in the long ram pipe produced the reduced velocity near the outer wall characteristic of configuration B. This configuration is significant inasmuch as it is representative of the inlet-air duct geometry used for most investigations in the Lewis altitude wind tunnel. For configuration C, the velocity distribution parameter varied by 0.59 across the annulus, and the slope of the velocity parameter curve was considerably greater than for the other configurations. The corresponding velocity at the outside of the annulus was reduced to approximately 0.71 of the velocity at the spinner.

Inasmuch as the distortions obtained with the first engine were such that the velocities were highest near the first-stage

blade roots, data were desired during the second phase of the investigation with the high velocities near the blade tips. In order to produce such a distribution, an annular screen 4 inches high was installed on the engine spinner to form configuration E. The resulting curve for configuration E (fig. 7) indicates that very low velocities existed near the first-stage blade roots. Owing to the uncertainty of the static pressures, the magnitude of the distortion obtained is expressed in terms of the total pressures, which varied by 103 pounds per square foot across the annulus and correspond to a variation of 14.2 percent of the average total pressure available at an altitude of 30,000 feet. A dashed line was used to denote the distribution near the outer wall because the three values used in obtaining the average at 96 percent of the annulus width scattered considerably.

For the three configurations used with the first engine, the velocity-distribution parameter downstream of the engine-inlet screen is presented in figure 8. Values of the velocity-distribution parameter were reduced considerably (fig. 8(a)) at 24 and 92 percent of the annulus width. The total-pressure tubes located at these radii were apparently in the wake of the circular elements of the engine screen. The velocity-distribution parameter, as measured by all tubes, is given in figure 8(a), and in figure 8(b) without the values at 24 and 92 percent of the annulus width. The effect of the engine-inlet screen on the velocity distribution is indicated by a comparison of the data obtained upstream (fig. 7) and downstream (fig. 8(b)) which shows that the engine-inlet screen tends to reduce the distortions slightly.

The radial velocity distribution at the compressor outlet for the various configurations is given in figure 9(a) for the first engine and in figure 9(b) for the second engine. The inlet distortions produced by the ram pipe with or without spoilers did not persist through the compressor (fig. 9(a)). Data obtained with the second engine (fig. 9(b)) show that even the severe radial distortion obtained with the inner ring (configuration E) did not persist through the compressor. For both engines, the random variations in distribution obtained with the various inlet configurations were much smaller than the variations produced by the compressor.

Circumferential variations in the velocity distribution at the engine inlet at approximately 45 percent of the annulus width as measured from the root of annulus are shown in figure 10. The distribution obtained for configuration A was very uniform and the slight variations obtained with configurations B and D are considered

insignificant in view of the much larger variations in the radial direction. The distributions for configurations C and E are not shown inasmuch as they were similar to those for B and D, respectively. Two very marked regions of low velocity were obtained by installing the two screen segments in the bellmouth (configuration F). The variation in velocity-distribution parameter of 0.78 for configuration F (fig. 10) corresponds to a total-pressure variation of 90 pounds per square foot. The instrumentation at the compressor outlet was not sufficiently extensive to determine accurately the circumferential pressure distribution, but an indication of the tendency of these circumferential distortions to persist or disappear in passing through the compressor was obtained by a study of the combustor temperature balance. This balance was indicated by thermocouples located on the center line of each combustor just downstream from the turbine. A comparison of the burner balance obtained at the same operating conditions with and without the screen segments installed indicates that the distortions tend to disappear in passing through the compressor.

Compressor characteristics. - Inasmuch as the disturbances in the engine-inlet air-flow pattern are not transmitted beyond the compressor in a consistent manner and the resulting variations that do occur at the compressor outlet are small compared with the change produced by the compressor, the primary effects on over-all engine performance are attributable to changes in compressor performance. Compressor-characteristic curves obtained at an altitude of 25,000 feet with the bellmouth and ram pipe (with and without spoilers) attached to the first engine are given in figure 11. Similar curves for configurations used with the second engine at an altitude of 30,000 feet are given in figure 12. The air flows are presented as ratios, based on the air flow obtained at rated engine speed with a uniform inlet-air-flow pattern.

As shown by the data of figure 11 and similar data for other altitudes, the air flow was not appreciably affected by distortions of the severity obtained with configurations B and C. The only effect appears at 78.5 percent of rated speed, where for a given pressure ratio the air flow was slightly higher with the uniform engine-inlet velocity distribution over most of the range of compressor-pressure ratios investigated.

The data for the more severe distortions used with the second engine show that, for a common average value of total pressure downstream of the obstructions, the air-flow ratio was 0.01 to 0.04 higher for the configurations having obstructions in the inlet (fig. 12). In view of this unexpected result and also the uncertainty

of static-pressure measurement at station 1, air-flow values for configuration F were checked and found to be correct by comparing the combustion efficiencies with those obtained with configuration D. This comparison constitutes a reliable check on air-flow values inasmuch as all other quantities entering the combustion-efficiency equation were substantiated by interplotting. It would be expected that, for a common total pressure upstream of the obstructions, equal or lower air flows would be obtained for operation with the obstructions installed. Air-flow values were therefore calculated by use of the factors δ and θ for the same total pressure upstream of the obstructions; the resulting air flows were slightly lower with the obstructions installed.

The increased flow with the obstructions, based on a common average value of total pressure downstream of the obstructions, may be corroborated to some extent by the observation, based on data from a previous investigation, that the air flow increases at a slightly faster rate than the total pressure at station 1. Accordingly, the higher total pressure in the unobstructed areas of the compressor face would produce slightly more than a proportionate increase in flow whereas the converse is true of the regions behind the obstructions, with the net result a slight increase in air flow. This effect, coupled with the experimental error of the measurements, probably accounts for the variations in mass flow shown.

Compressor efficiencies, based on measurements at stations 1 and 3, are presented in figures 13 and 14 for the first and second engines, respectively. For configurations A, B, and C, slightly higher compressor efficiencies were obtained for most operating conditions with the uniform inlet-velocity distribution; the total variation, however, was approximately the same magnitude as the probable error of the measurements. Slightly higher efficiencies were similarly obtained with the uniform velocity distribution at the inlet of the second engine. The maximum decrease in compressor efficiency of 0.024 resulted from the distortion imposed by configuration B at an altitude of 50,000 feet and 0.913 rated engine speed. The lower level of compressor efficiencies obtained with the first engine is attributed largely to the pressure drop across the standard engine screen, which decreases the compressor-pressure ratio.

Over-all engine performance. - From the pumping-characteristic curves, the net thrust and specific fuel consumption of the engine operating under the various conditions imposed by the inlet configurations were calculated for a common average total pressure downstream of the obstructions at station 1. The engine performance

variations reflect only the effects of the distortions on the internal aerodynamics of the engine and do not consider the effects of losses in rampressure associated with the various distortions.

By an analysis of the Brayton cycle upon which the engine operates, it can be shown that a decrease in compressor efficiency will result in a decrease in the engine-pressure ratio for a given engine-temperature ratio. Because the thrust values presented are based on fixed values of engine-temperature ratio, a reduction in compressor efficiency is reflected in reduced thrust as a result of lower engine-pressure ratio (equations (3) and (4) of appendix).

Thrust values shown in figures 15 and 17 are presented as ratios; the thrusts obtained with the distorted air-flow patterns are divided by the thrust obtained at the same operating conditions with a uniform distribution. At rated engine speed the thrusts obtained with the bellmouth and with the ram pipe, with spoilers, varied less than 2.0 percent, irrespective of altitude (fig. 15). The maximum variation with thrust was a decrease of 5.0 percent with configuration C at 91.3 percent of rated speed and an altitude of 50,000 feet. These thrust values follow the trend of compressor efficiencies shown in figure 13. Thrust values are believed to be accurate to approximately ±1 percent at rated engine speed for the lower altitudes and ±2 or 3 percent at the lower engine speeds and higher altitudes. At the lowest engine speed and an altitude of 50,000 feet, the pumping-characteristic curves could not be faired with enough certainty, owing to data scatter, to permit comparison.

Net-thrust specific fuel consumptions (fig. 16) are also presented as ratios, based on the engine performance with a uniform inlet air-flow distribution. These curves reflect not only the variations in net thrust shown in figure 15, but also any minor changes in combustion efficiency that result from the inlet air-flow distortions. The maximum variation in specific fuel consumption was 4.0 percent at 91.3 percent of rated engine speed and an altitude of 50,000 feet. At rated engine speed the maximum variation in specific fuel consumption was 2.5 percent and occurred at an altitude of 35,000 feet.

The effects of the large radial distortion obtained with the inner ring obstruction (configuration E) and the circumferential distortions obtained with the screen segments (configuration F) on the thrust and specific fuel consumption of the second engine are shown in figure 17. The thrust for configuration F was 1 to 3 percent higher than for the uniform inlet distribution at the higher

engine speeds and was slightly lower than for uniform distribution at the lowest engine speed. For configuration E, the thrust was 2 percent higher than for configuration D. The thrust curves of figure 17(a) reflect the changes in compressor efficiency and air flow.

The decrease in compressor efficiency coupled with slight changes in combustion efficiency for configuration F resulted in increases of from 1 to 3 percent in the net-thrust specific fuel consumption (fig. 17(b)) as compared with the values obtained with the uniform inlet-velocity distribution.

Throughout the investigation, vibration readings obtained in both vertical and horizontal planes at the compressor-outlet flange and the turbine flange were carefully observed. No noticeable increase in vibration occurred with any of the configurations, and all values were well within the limits specified by the manufacturer.

SUMMARY OF RESULTS

An investigation was conducted over a wide range of altitudes at a fixed flight Mach number in the NACA Lewis altitude wind tunnel to determine the effect of inlet-air distortion on the performance of a full-scale axial-flow turbojet engine.

For this investigation, radial total-pressure variations of 103 pounds per square foot and circumferential variations of 90 pounds per square foot at an altitude of 30,000 feet and a nominal flight Mach number of 0.21 were obtained.

For some of the configurations and operating conditions investigated, the effect of distortions of the inlet-velocity pattern on the internal aerodynamics of the engine resulted in slight improvements in performance; at other operating conditions the performance was slightly impaired. These effects are distinct from the performance losses associated with losses in ram-pressure recovery. In general, compressor efficiencies were reduced slightly by the nonuniform inlet-velocity distributions. For the extreme distortions of the inlet-velocity pattern, the air flows were slightly higher than for the uniform inlet configuration. With the inlet-velocity distortions investigated, the net thrust varied between 0.95 and 1.03 of the net thrust with the uniform inlet configuration at the same operating conditions. Similarly, the ratio of specific fuel consumption values varied from 1.00 to 1.04. It may therefore be

concluded that performance changes due to the effects of non-uniform inlet velocity on the internal aerodynamics of the engine investigated were not serious for the range of distortions investigated.

Lewis Flight Propulsion Laboratory,
National Advisory Committee for Aeronautics,
Cleveland, Ohio.

APPENDIX - CALCULATIONS

Symbols

The following symbols are used herein:

A	cross-sectional area, sq ft
F_n	net thrust, lb
g	acceleration due to gravity, 32.2 ft/sec^2
P	total pressure, lb/sq ft absolute
p	static pressure, lb/sq ft absolute
q	velocity head, lb/sq ft
R	gas constant, 53.3 ft-lb/(lb)($^\circ$R)
T	total temperature, $^\circ$R
T_i	indicated temperature, $^\circ$R
t	static temperature, $^\circ$R
V	velocity, ft/sec
W_a	air flow, lb/sec
W_f	fuel flow, lb/sec
γ	ratio of specific heats
δ	ratio of absolute total pressure at engine inlet to absolute static pressure of NACA standard atmosphere at sea level
η_c	adiabatic compressor efficiency
θ	ratio of absolute total temperature at engine inlet to absolute static temperature of NACA standard atmosphere at sea level

Subscripts:

0	free air stream
1	engine inlet
2	compressor inlet behind screen
3	compressor outlet
4	turbine outlet
5	exhaust-nozzle inlet
av	average
j	jet
l	local

Methods of Calculation

Thrust and air flow. - The thrust of a turbojet engine is a function of the air flow, engine-temperature ratio, and engine-pressure ratio. Air flows for configurations A, B, C, D, and F were calculated from the pressure and temperature survey at the engine inlet (station 1) by use of the following equation:

$$W_a = A_1 p_1 \sqrt{\frac{2\gamma_1 g}{(\gamma_1 - 1)Rt_1}\left[\left(\frac{P_1}{p_1}\right)^{\frac{\gamma_1 - 1}{\gamma_1}} - 1\right]} \qquad (1)$$

The relation between static and indicated temperatures is given by

$$t = \frac{T_i}{1 + 0.85\left[\left(\frac{P}{p}\right)^{\frac{\gamma - 1}{\gamma}} - 1\right]} \qquad (2)$$

where the value of 0.85 is an experimentally determined thermocouple impact recovery factor.

As previously mentioned, the air-flow values obtained from measurements at station 1 were unreliable for configuration E due apparently to a nonuniform static-pressure distribution. Inasmuch as distortions at the engine inlet do not appear to persist beyond the compressor, the combustion efficiency should be approximately the same for all configurations at a given engine speed and pressure level. Also regardless of changes in the component efficiency, the enthalpy rise of the air through the compressor must equal the enthalpy drop through the turbine for any steady-state operating condition. As a result, a plot of engine total-temperature rise as a function of engine fuel-air ratio should be about the same for configurations D and E. Such a plot was made with the data for configuration D for which the air-flow measurements at station 1 were satisfactory. Using this plot in conjunction with the measured values of temperature rise (T_5-T_1) and fuel flow for configuration E, the air flow for configuration E was obtained.

The thrust of the engine can be expressed by the following equations:

$$F_n = \frac{W_a}{g} (V_j - V_0) \tag{3}$$

where the momentum of the fuel is ignored,

$$V_j = \sqrt{\frac{2\gamma_5}{\gamma_5-1} gRT_5 \left[1 - \left(\frac{p_0}{P_5}\right)^{\frac{\gamma_5-1}{\gamma_5}}\right]} \tag{4}$$

and

$$V_0 = \sqrt{\frac{2\gamma_1}{\gamma_1-1} gRT_1 \left[1 - \left(\frac{p_0}{P_1}\right)^{\frac{\gamma_1-1}{\gamma_1}}\right]} \tag{5}$$

Net thrust was obtained by the use of the pumping characteristic curves in conjunction with equations (1), (3), (4), and (5).

Compressor efficiency. - The equation for adiabatic compressor efficiency is

$$\eta_c = \frac{\left(\frac{P_3}{P_1}\right)^{\frac{\gamma-1}{\gamma}} - 1}{\frac{T_3}{T_1} - 1} \qquad (6)$$

Compressor efficiencies at the same flight conditions and compressor Mach number were plotted as a function of compressor pressure ratio; for the first engine there was no definite trend in the small range of pressure ratios investigated, but for the second engine there was a definite trend. Therefore, for the first engine the efficiency values presented represent the average of the data points at various compressor pressure ratios obtained by changing the exhaust-nozzle area. Efficiencies for the second engine were taken at compressor-pressure ratios corresponding to the value of engine-temperature ratio for a rated-area exhaust nozzle. All individual efficiencies averaged were within ±1.25 percent of the mean value. Compressor efficiencies were checked by a calculation that included the effects of the radial mass-flow distribution (and radial temperature gradients); the maximum correction for these effects, however, was only 0.7 percent.

REFERENCES

1. Sanders, Newell D., and Palasics, John: Analysis of Effects of Inlet Pressure Losses on Performance of Axial-Flow Type Turbojet Engine. NACA RM E8J25b, 1948.

2. Sanders, Newell D., and Behun, Michael: Generalization of Turbojet-Engine Performance in Terms of Pumping Characteristics. NACA TN 1927, 1949.

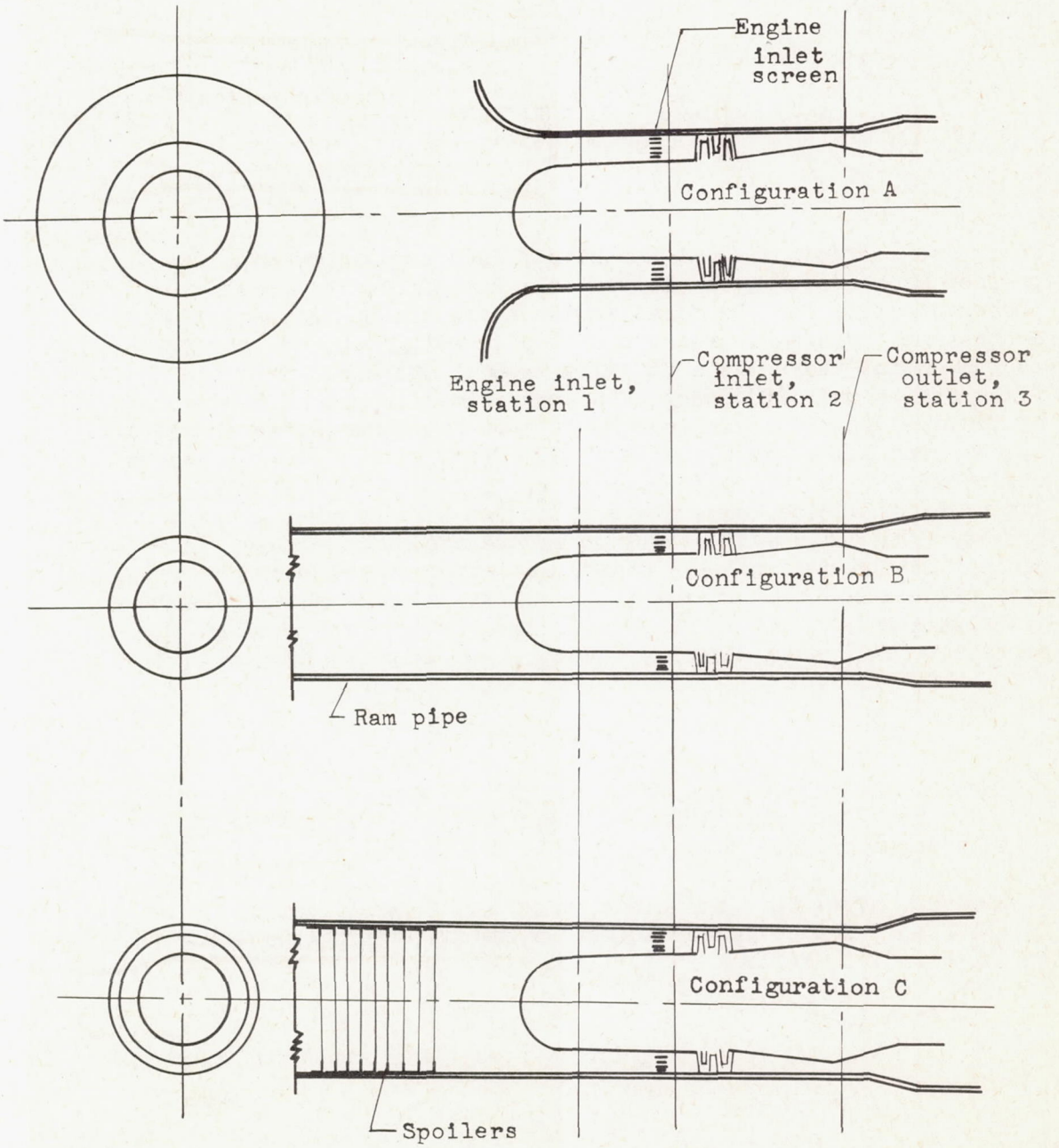

(a) First engine.

Figure 1. - Engine-inlet configurations.

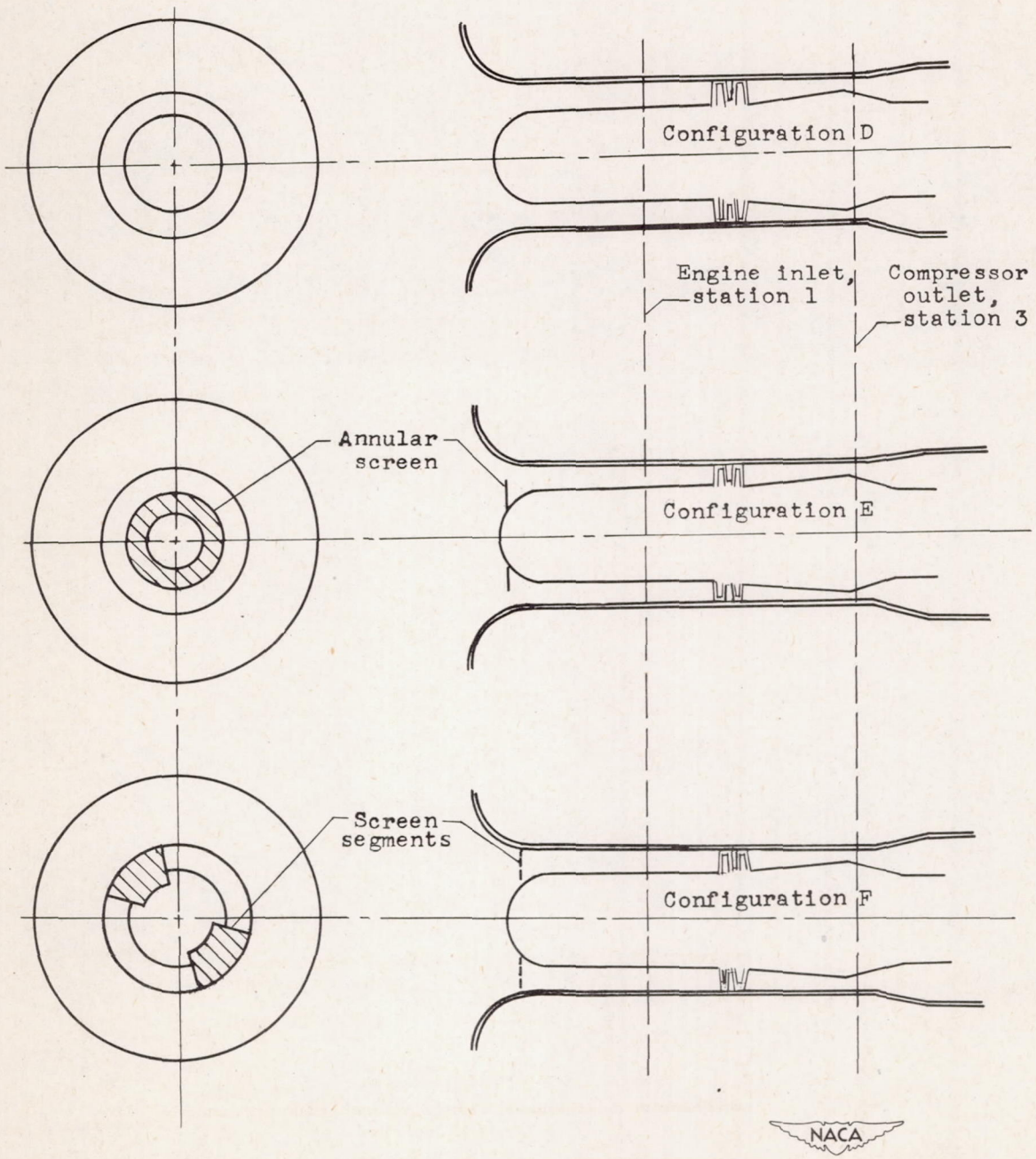

(b) Second engine.

Figure 1. - Concluded. Engine-inlet configurations.

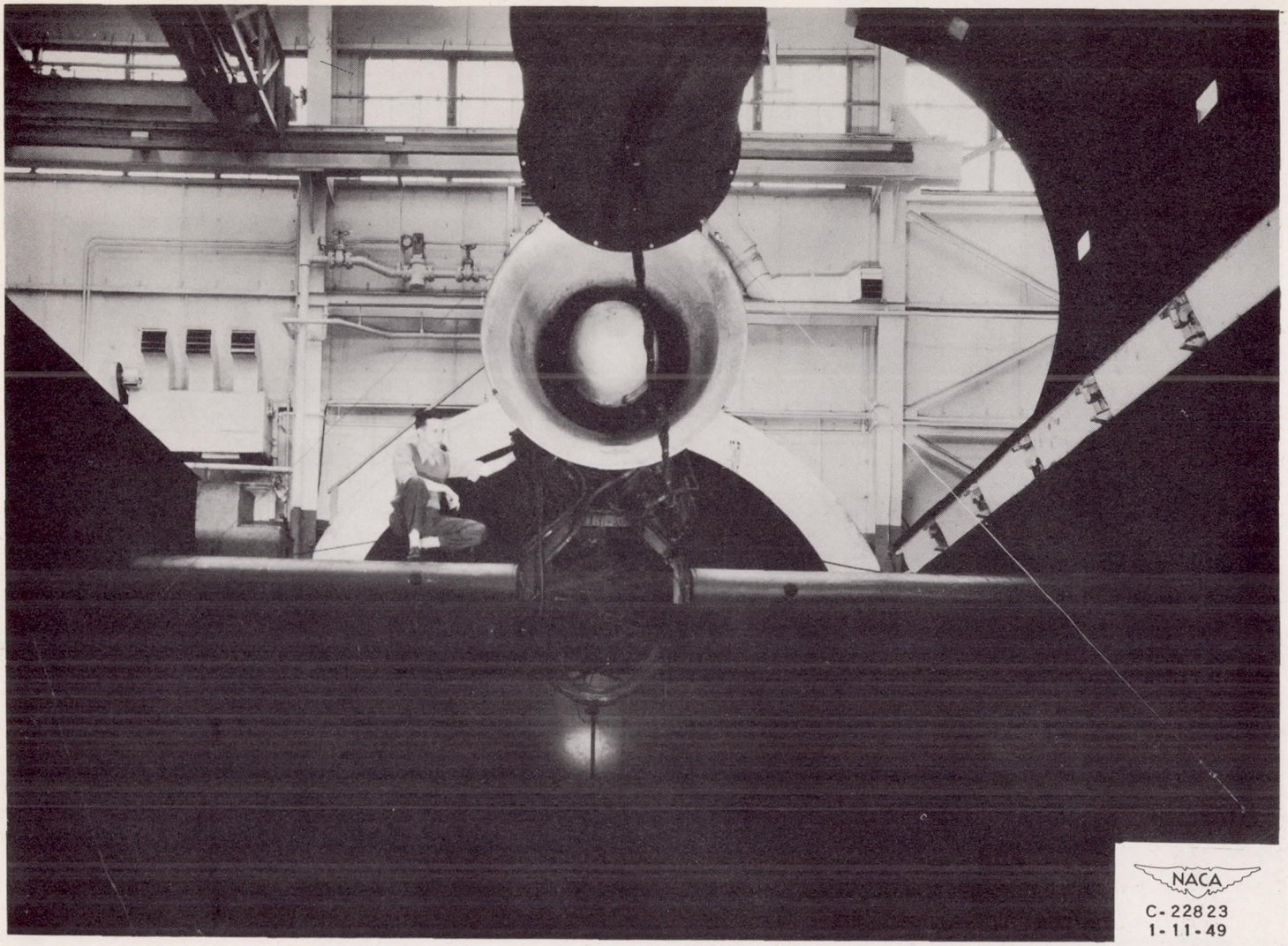

(a) Bellmouth entrance section installed on engine. Configuration A.

Figure 2. - Details of installation.

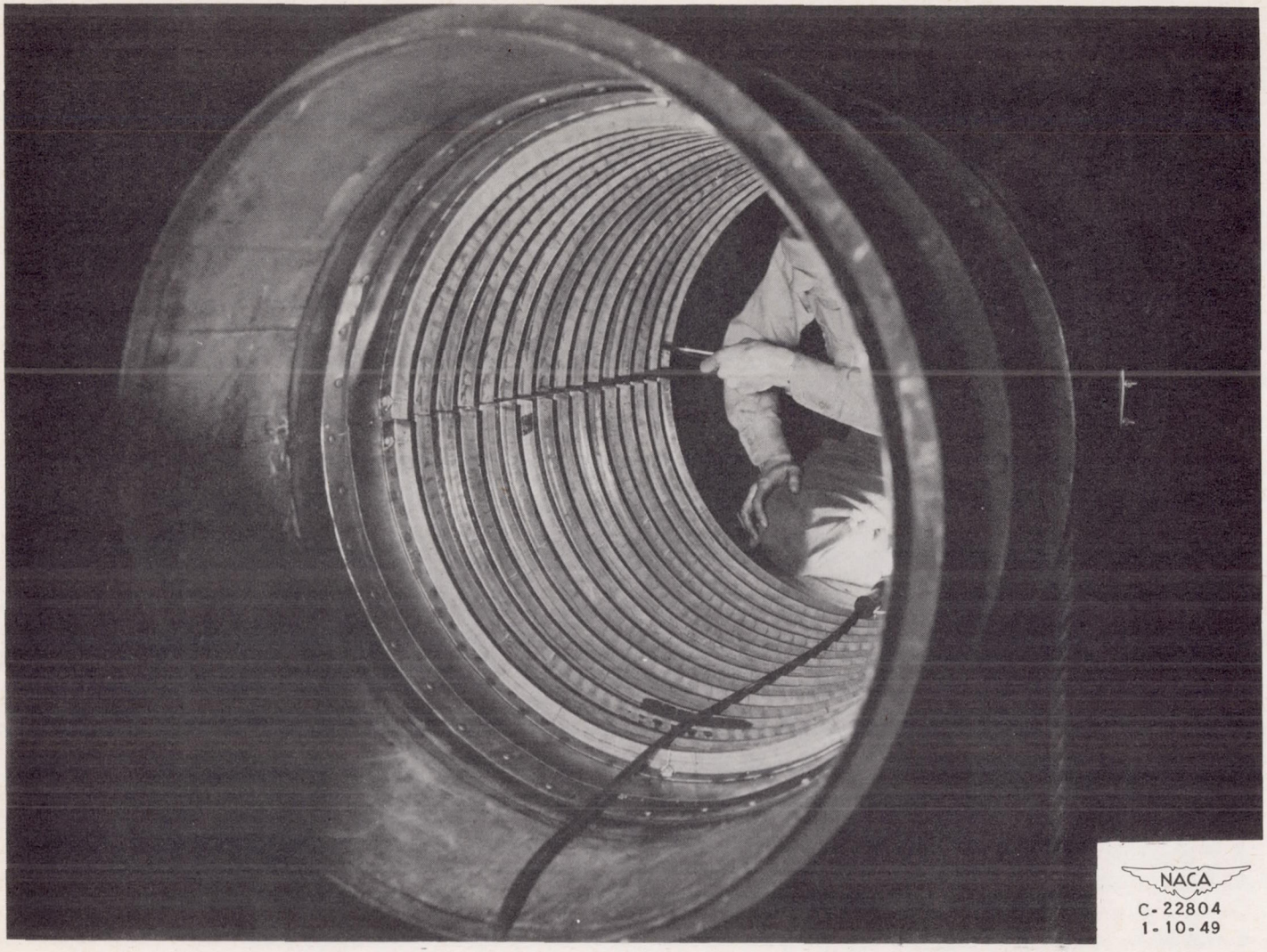

(b) Spoilers installed in ram pipe. Configuration C.

Figure 2. - Concluded. Details of installation.

Station	Total-pressure tubes	Static-pressure tubes	Wall static-pressure orifices	Thermocouples
First engine, configurations A, B, and C				
1	40	4	0	8
2	24	0	4	0
3	20	0	4	6
4	30	0	2	33
5	40	16	4	18
Second engine, configurations C, D, and E				
1	61	0	4	6
2	0	0	0	0
3	15	0	4	6
4	30	0	2	33
5	40	16	4	18

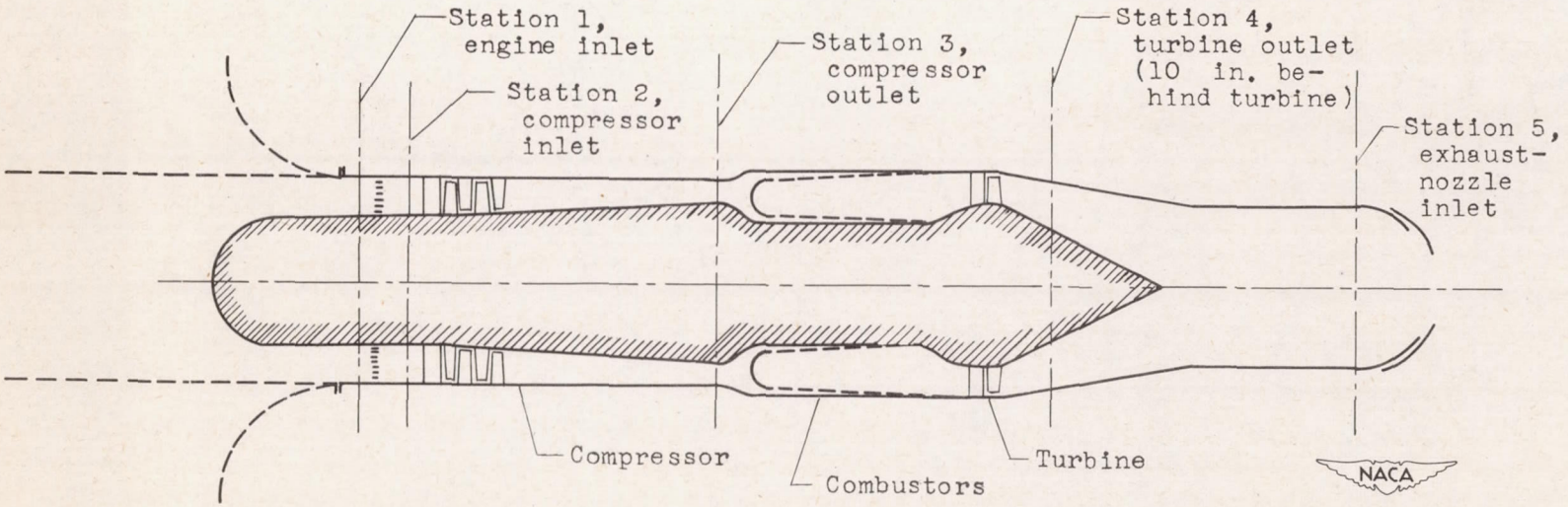

Figure 3. - Location of instrumentation surveys.

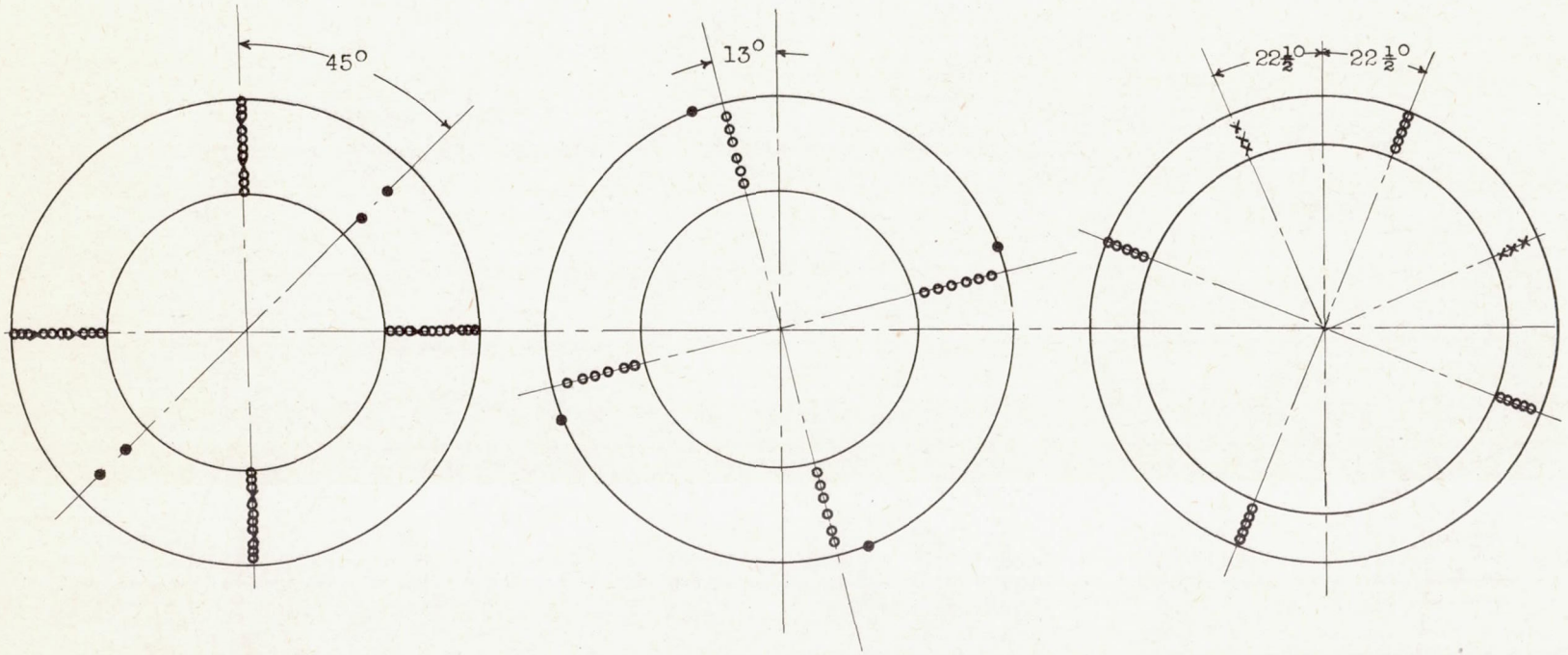

(a) First engine.

Figure 4. - Instrumentation viewed from upstream.

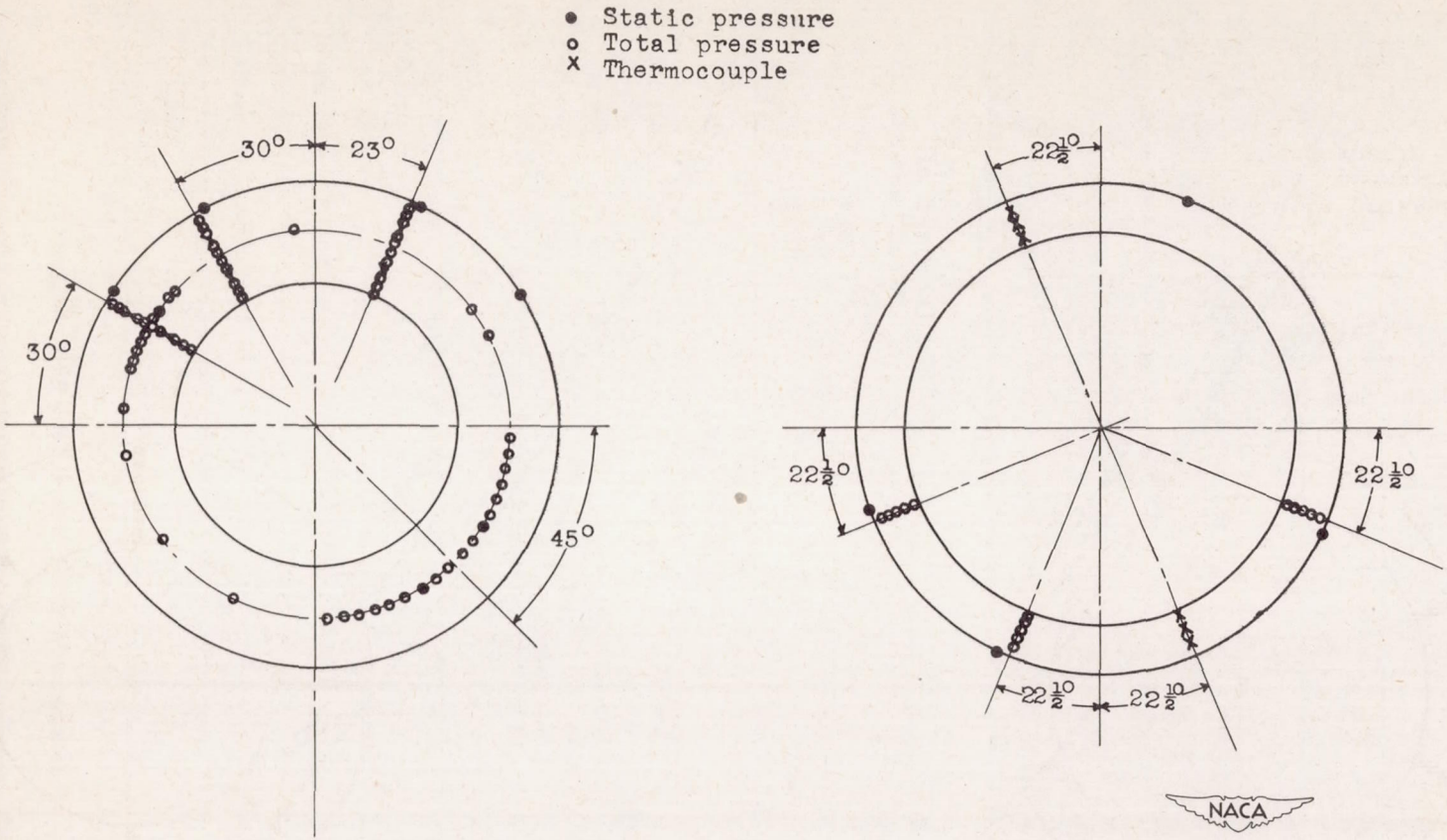

Engine inlet, station 1

Compressor outlet, station 3

(b) Second engine.

Figure 4. - Concluded. Instrumentation viewed from upstream.

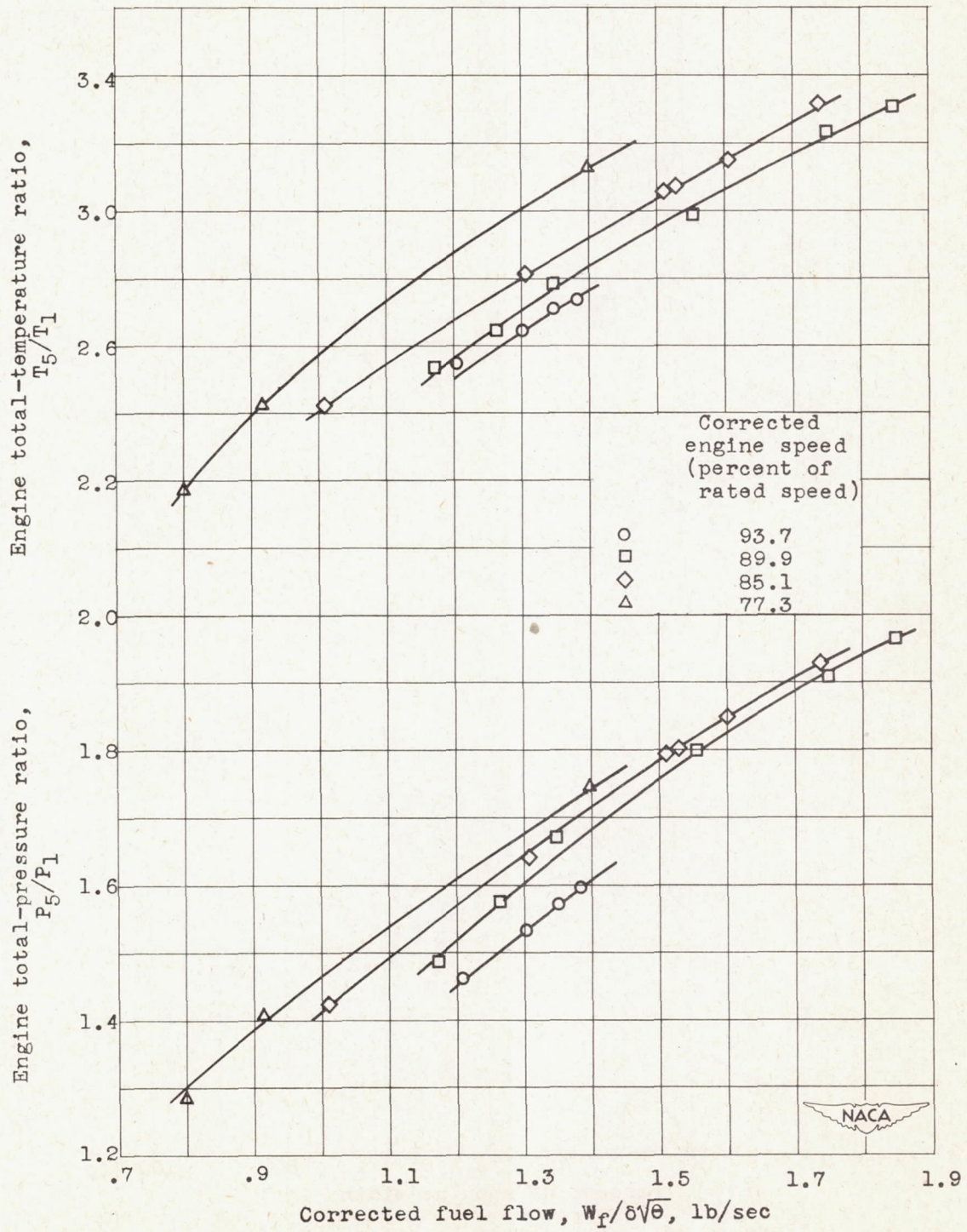

Figure 5. - Variation of engine total-temperature ratio and engine total-pressure ratio with corrected fuel flow. Configuration D; altitude, 30,000 feet.

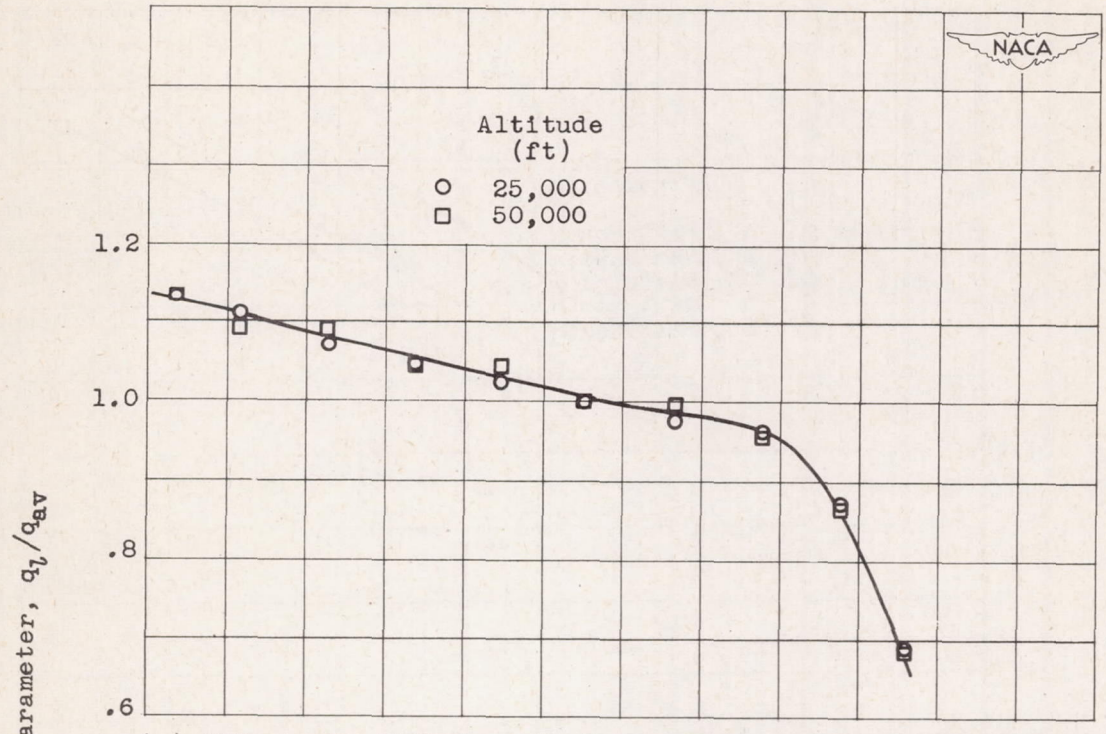

(a) Effect of altitude. 91.3 percent of rated engine speed.

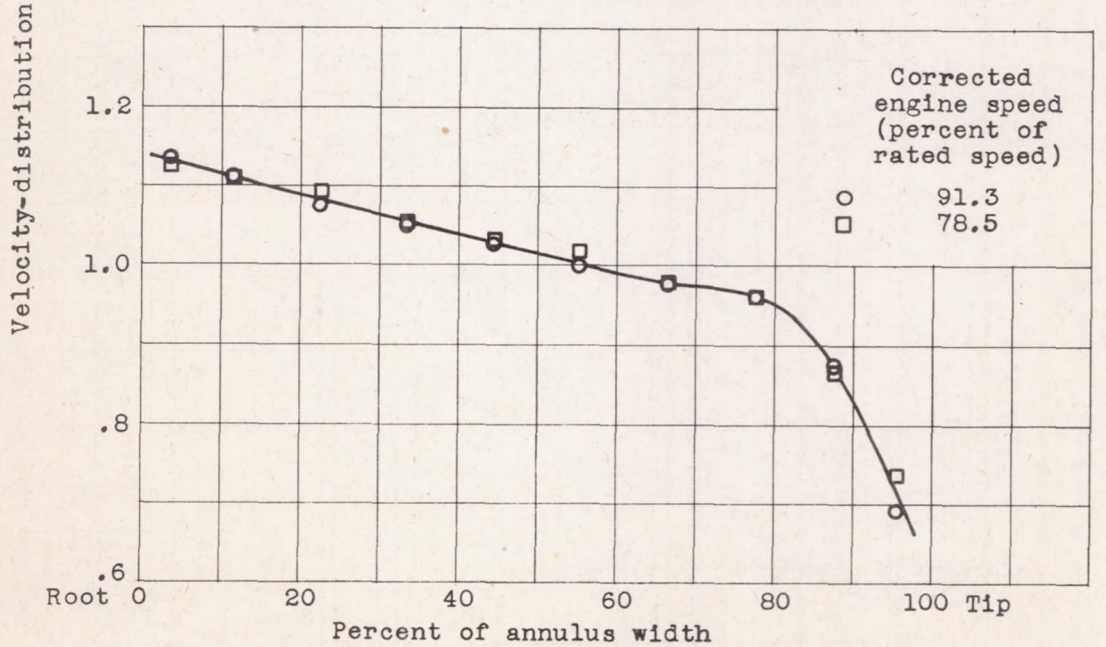

(b) Effect of engine speed. Altitude, 25,000 feet.

Figure 6. - Effect of altitude and engine speed on radial velocity distribution at engine inlet. Configuration B.

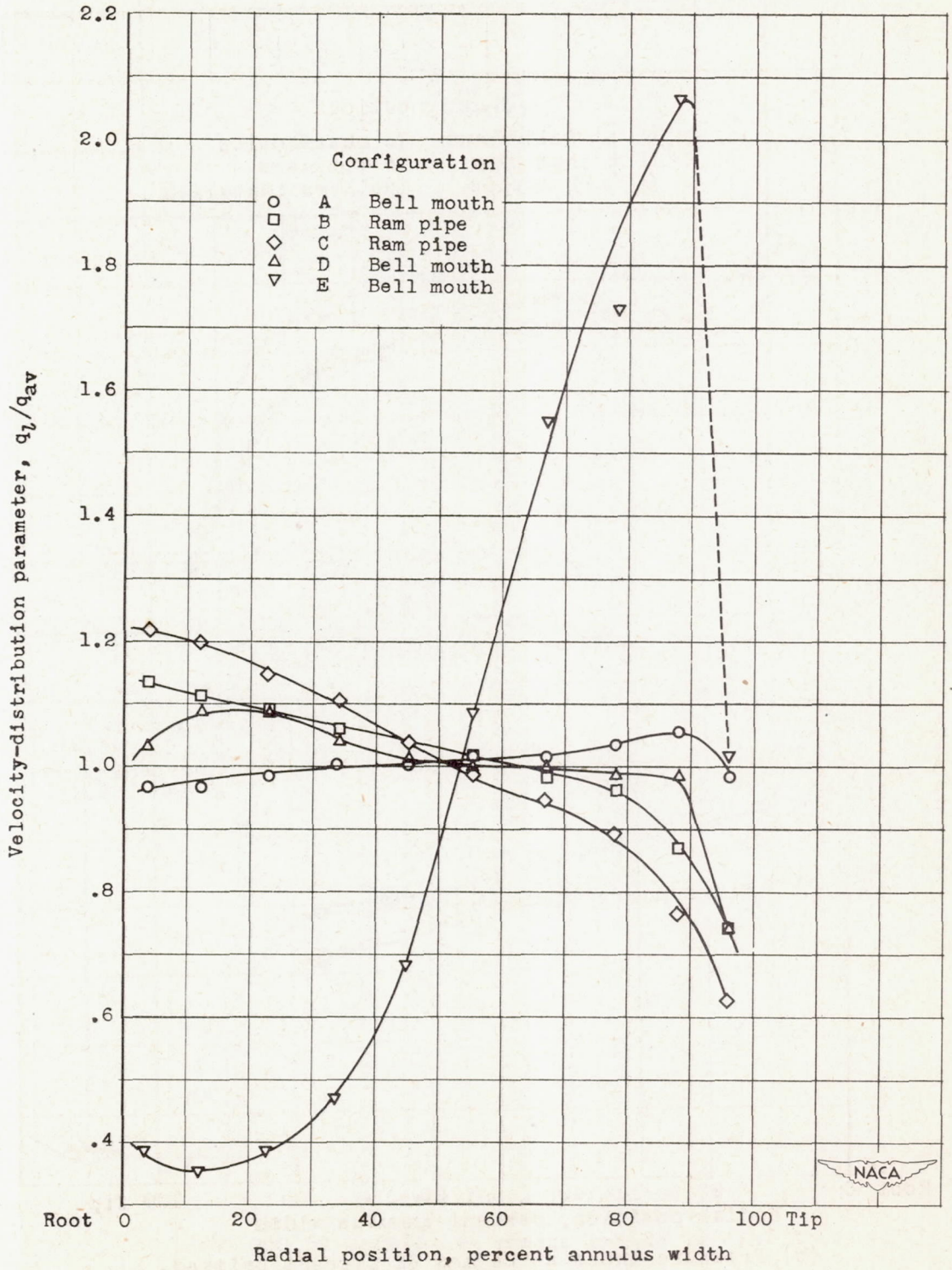

Figure 7. - Radial velocity distributions at engine inlet for configurations A, B, C, D, and E.

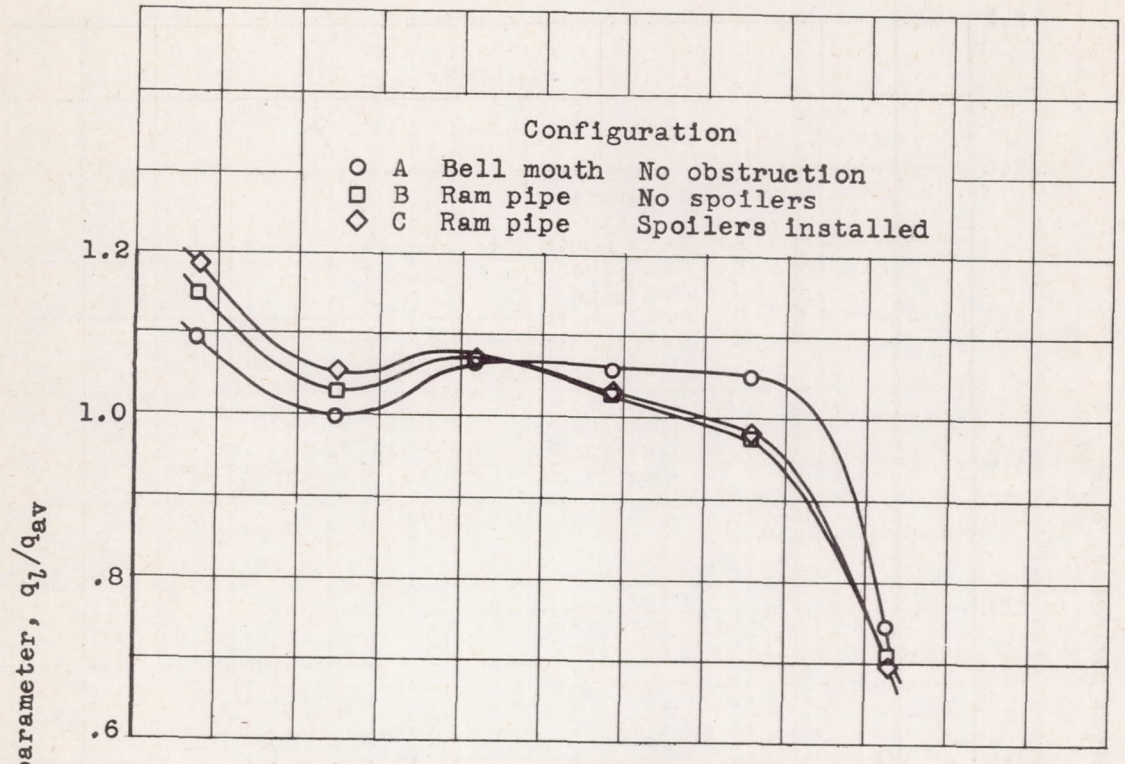

(a) All pressure tubes included.

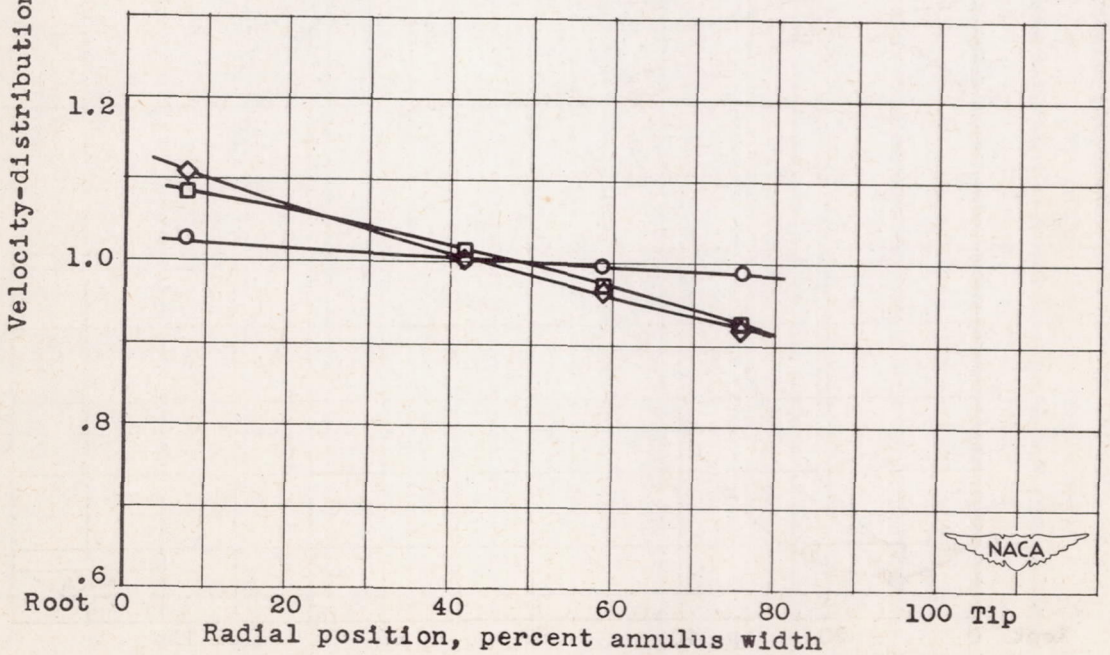

(b) Pressure tubes at 24 and 92 percent omitted.

Figure 8. - Radial velocity distribution at compressor inlet of first engine.

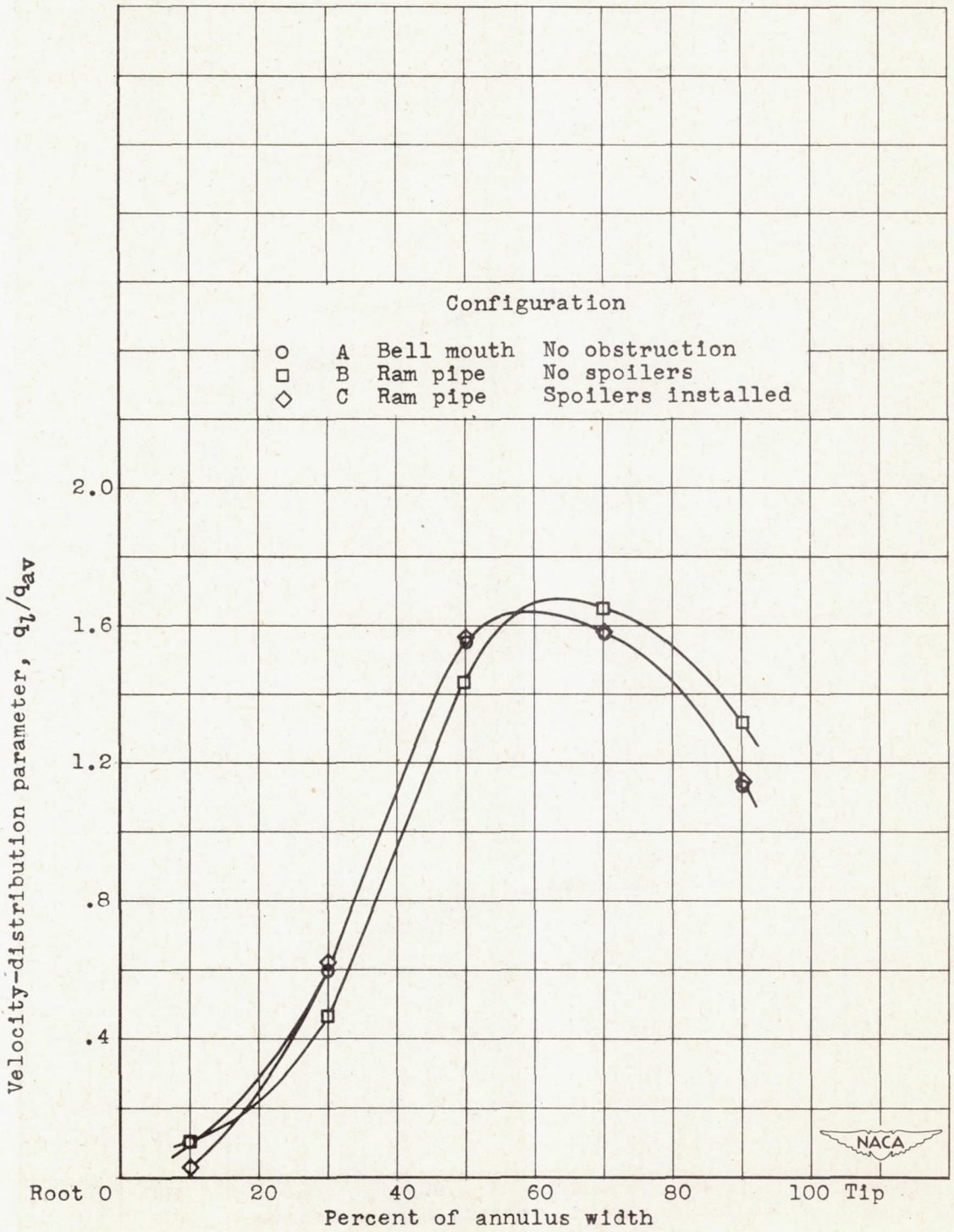

(a) First engine. 91.3 percent of rated engine speed.

Figure 9. - Velocity distribution at compressor outlet.

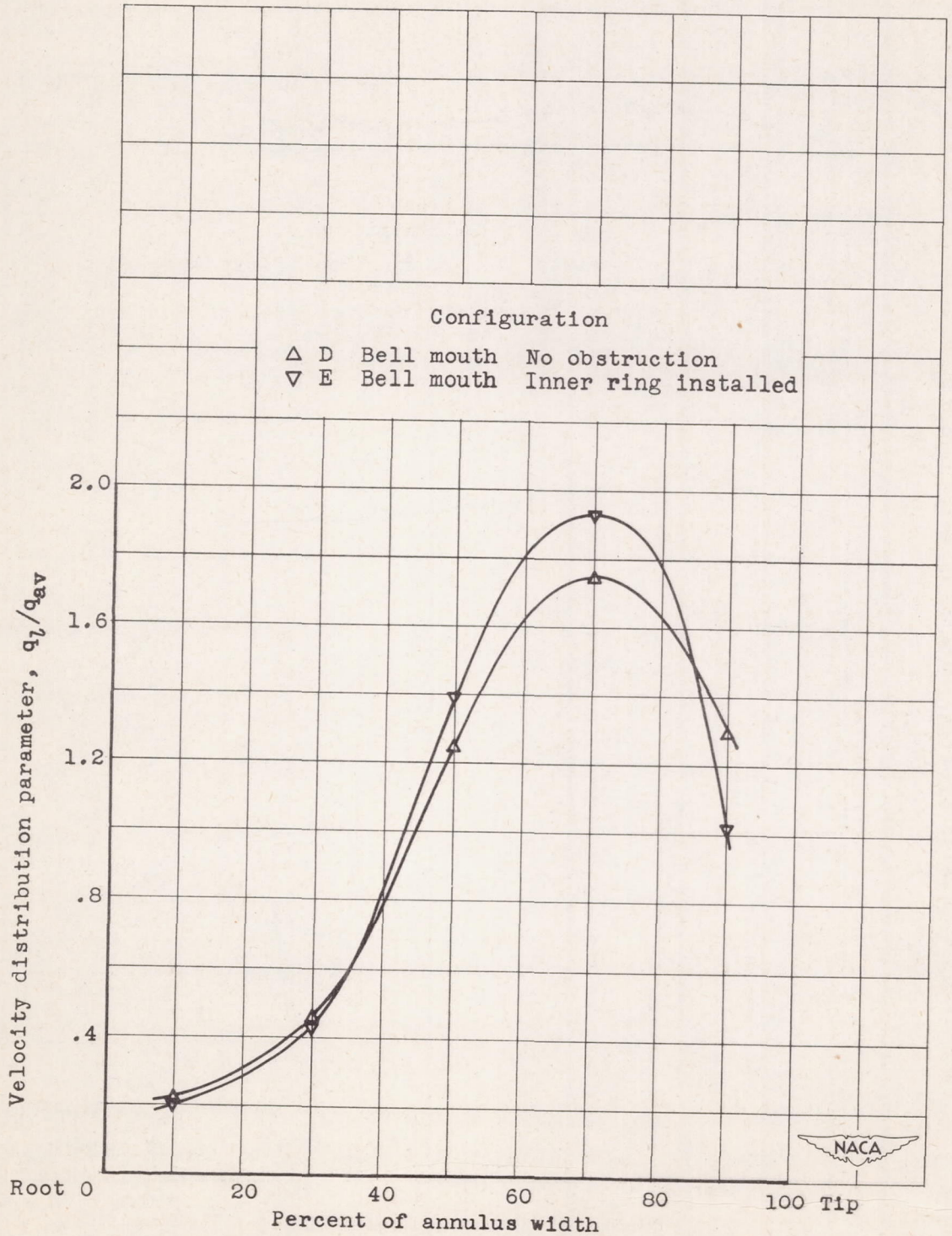

(b) Second engine; 77.3 percent of rated engine speed.

Figure 9. - Concluded. Velocity distribution at compressor outlet.

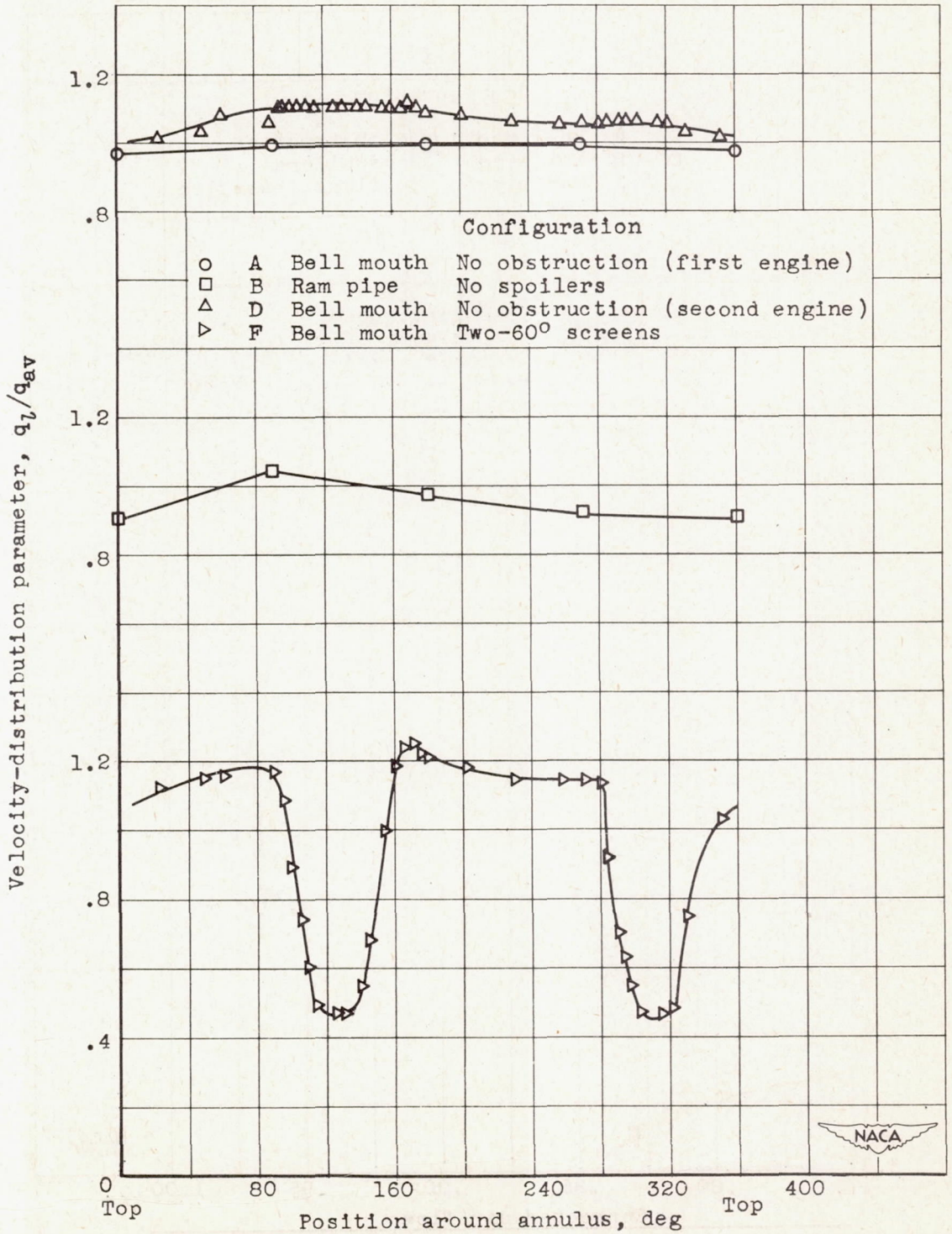

Figure 10. - Circumferential velocity distribution at engine inlet for configurations A, B, D, and F.

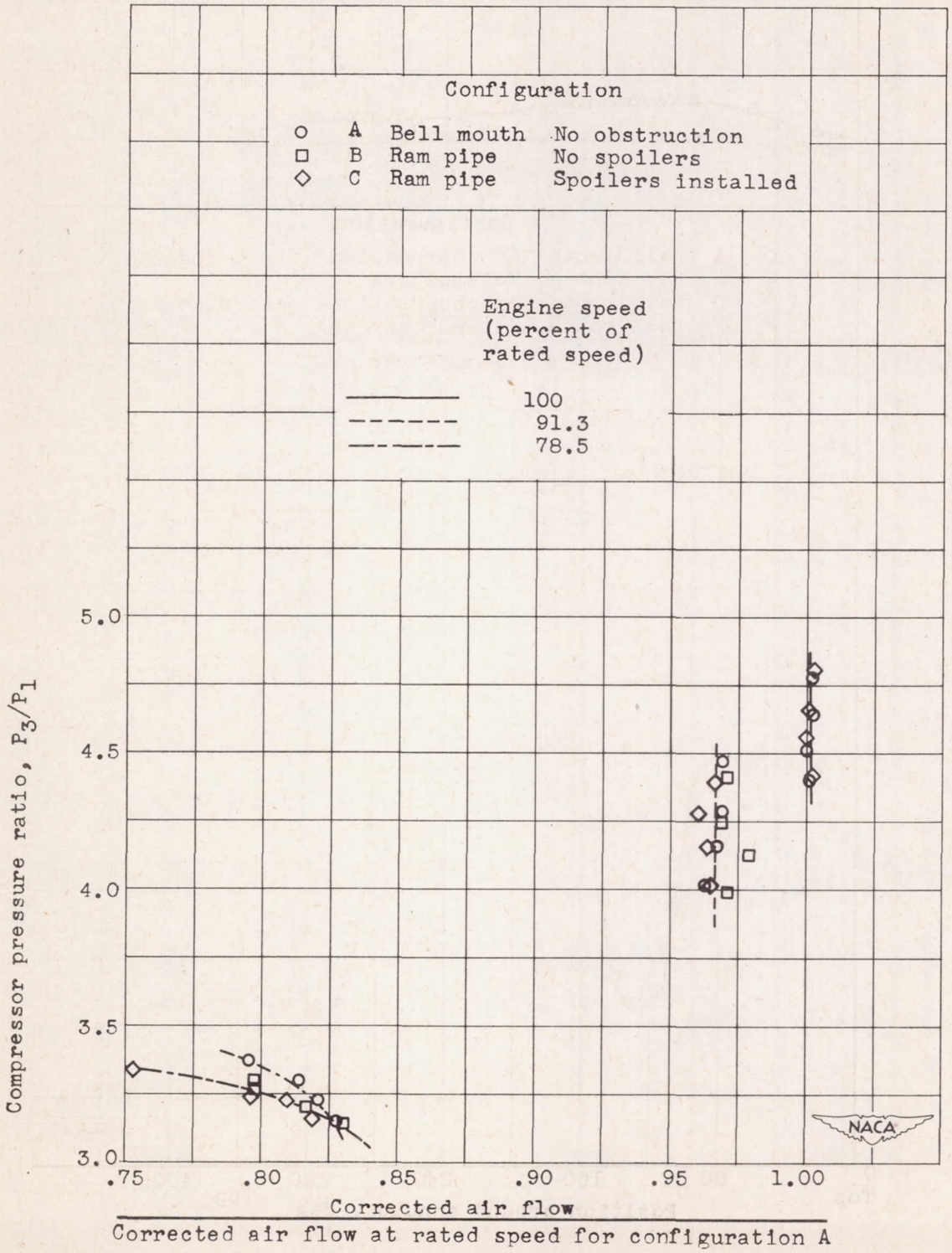

Figure 11. - Effect of engine-inlet velocity distribution on compressor characteristics of first engine. Altitude, 25,000 feet.

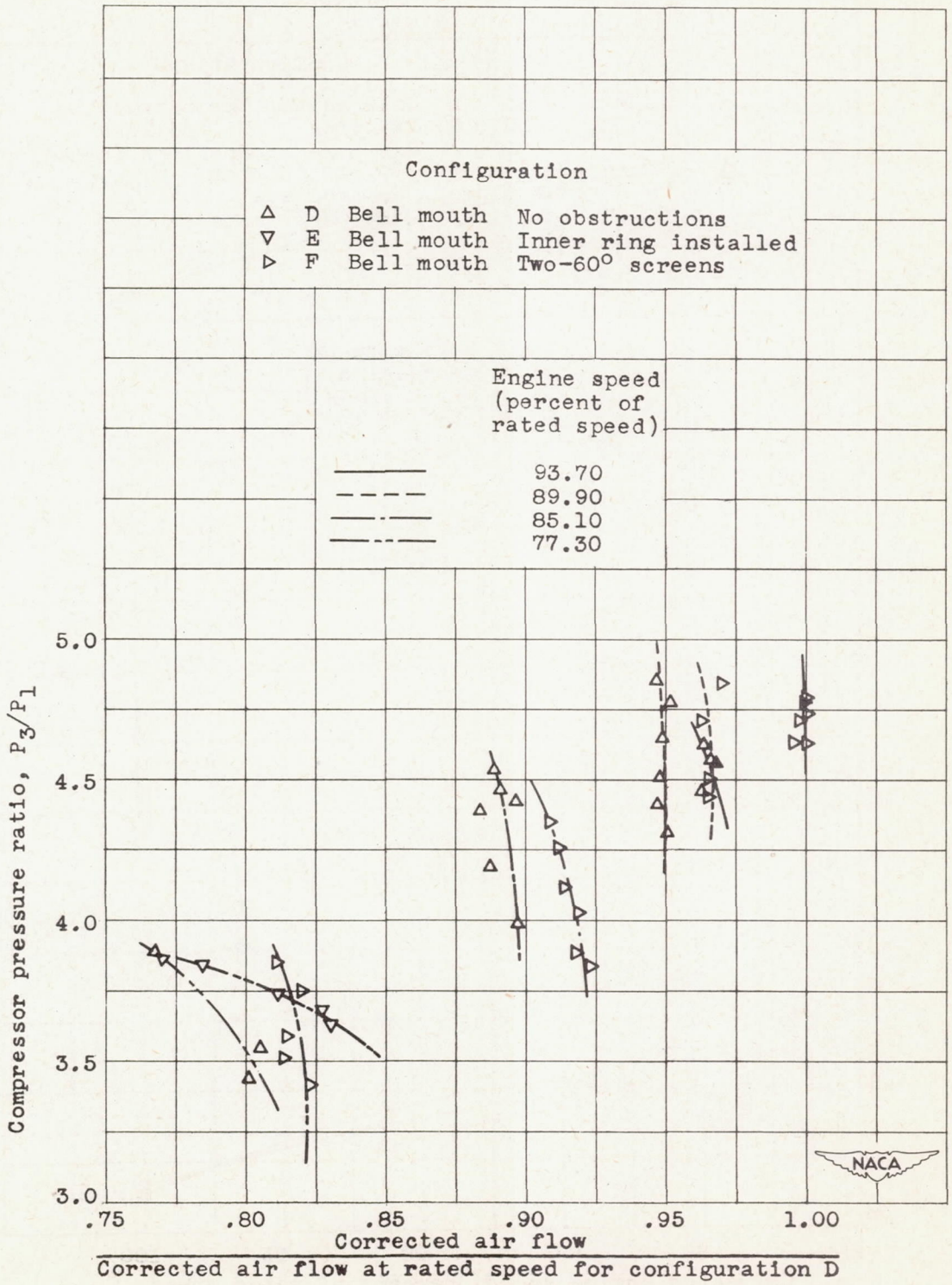

Figure 12. - Effect of engine-inlet velocity distribution on compressor characteristics of second engine. Altitude, 30,000 feet.

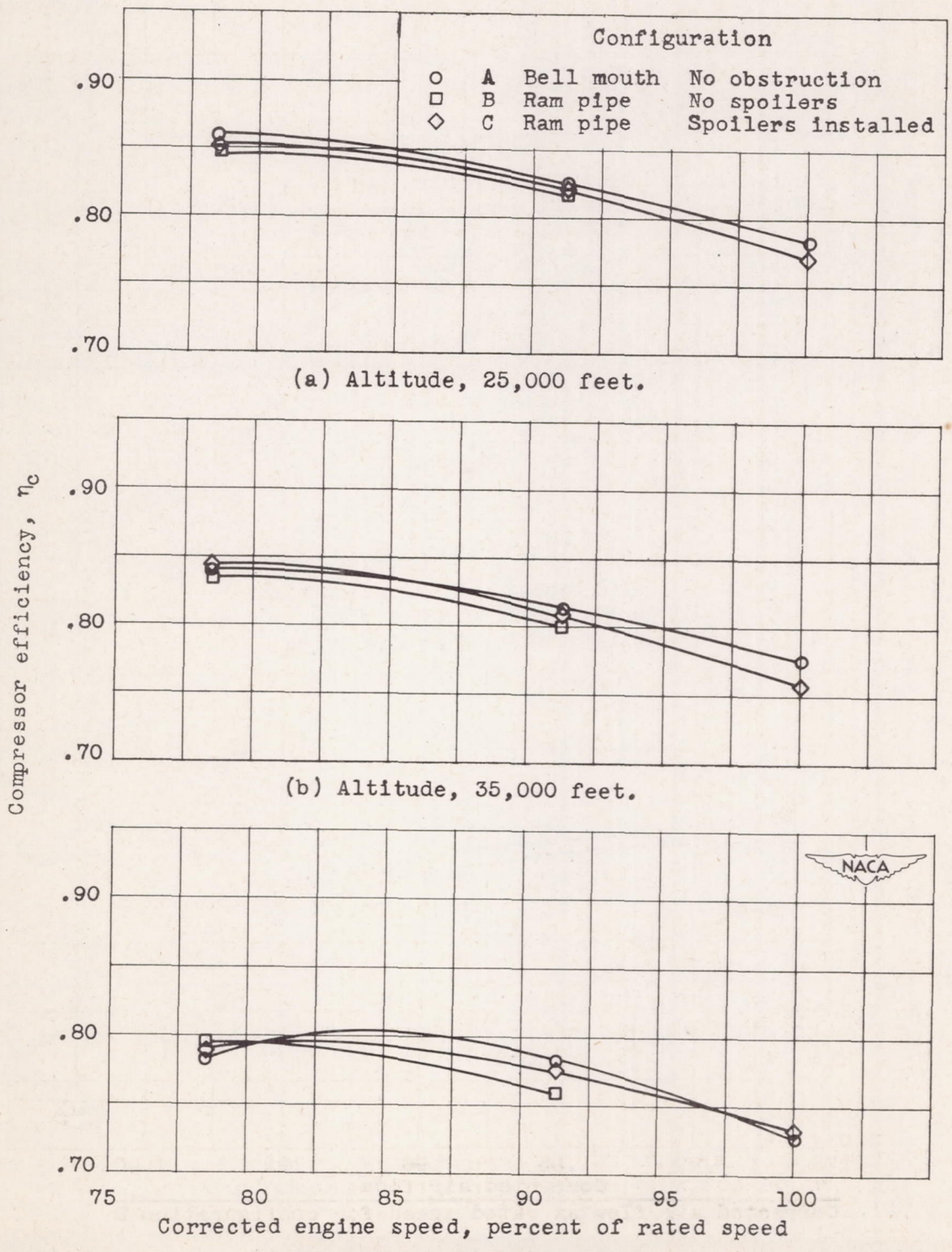

Figure 13. - Effect of engine-inlet-air velocity distribution on compressor efficiency of first engine.

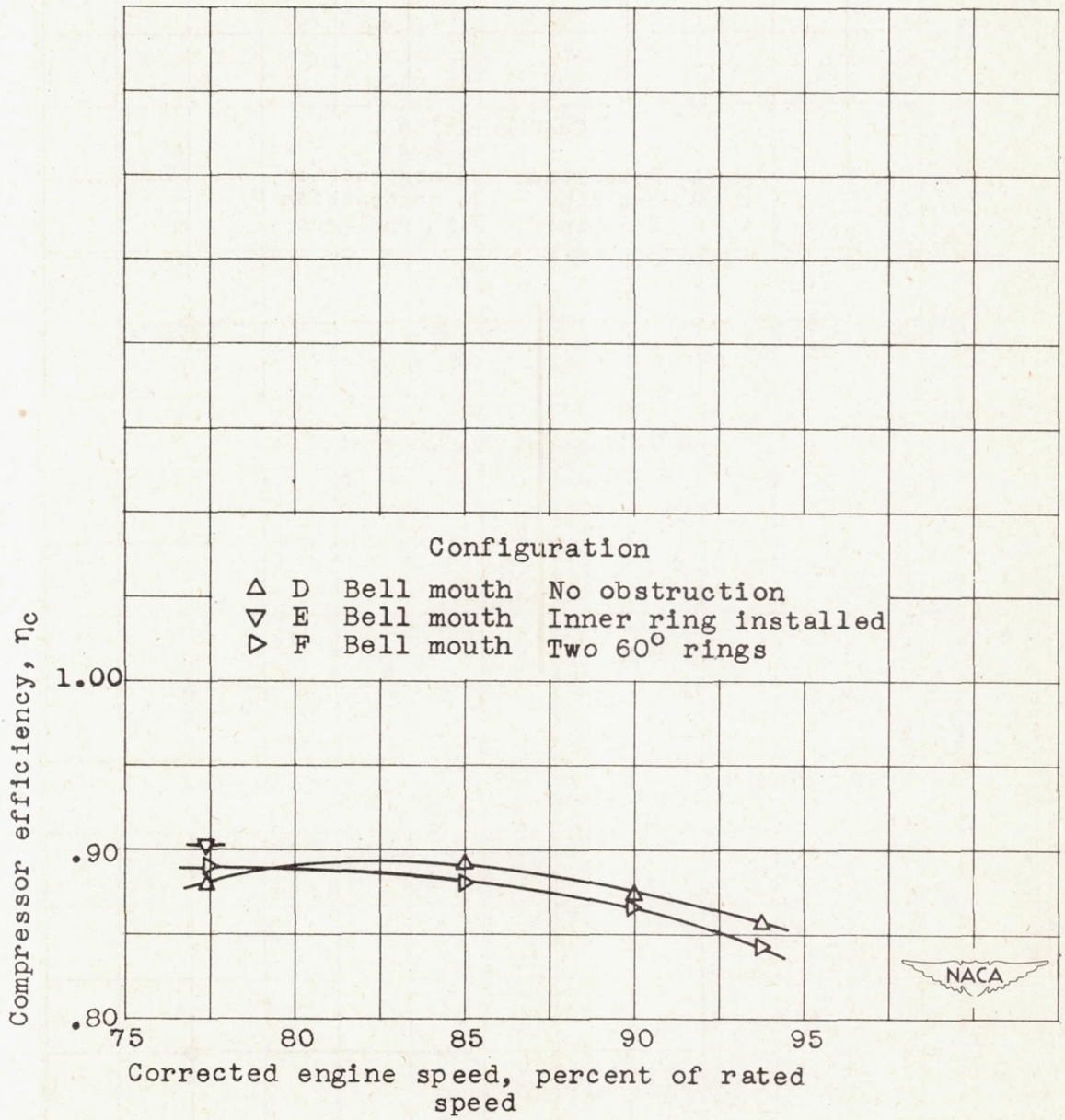

Figure 14. - Effect of engine-inlet-air velocity distribution on compressor efficiency of second engine. Altitude, 30,000 feet.

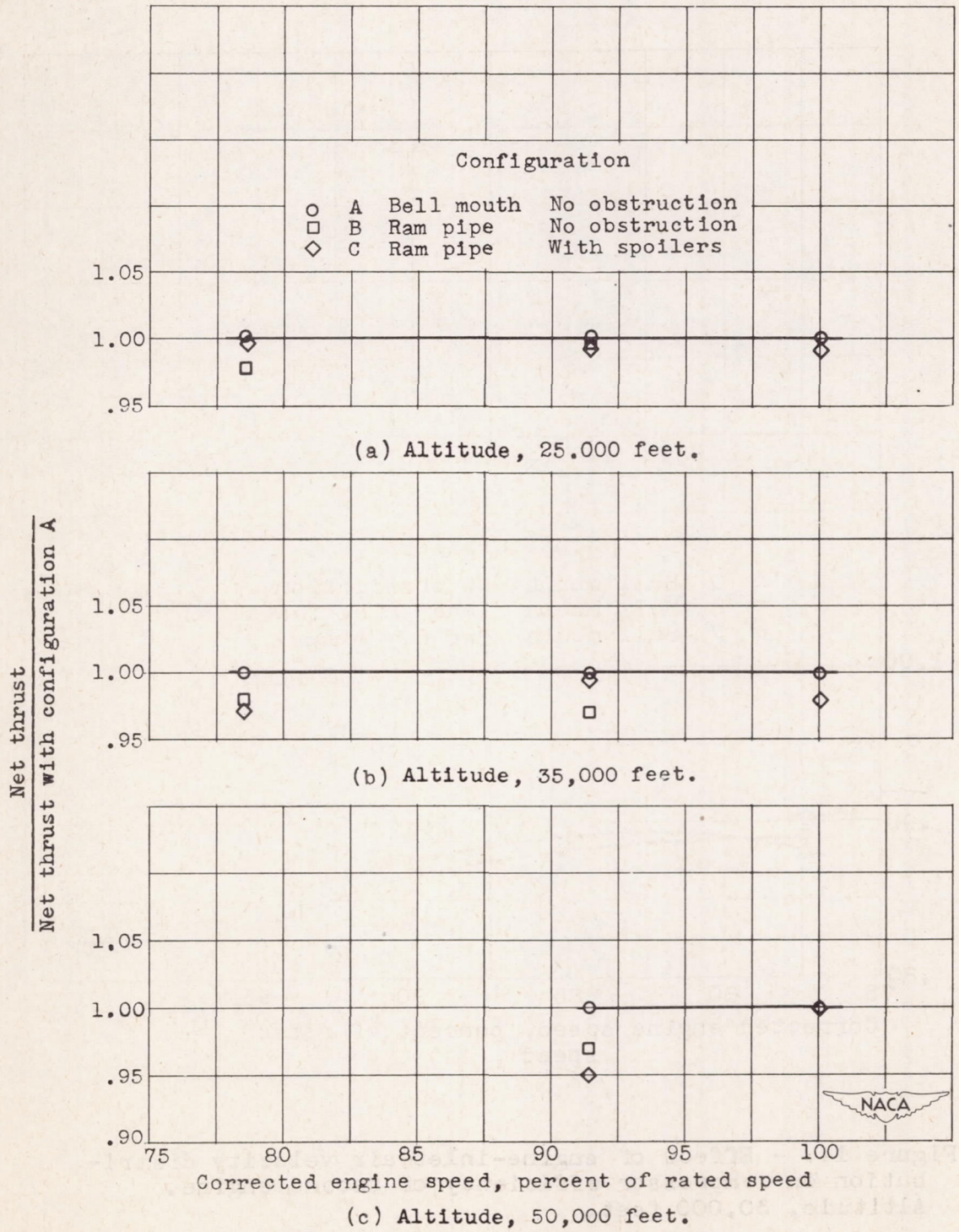

Figure 15. - Effect of engine-inlet-air velocity distribution on net thrust of first engine.

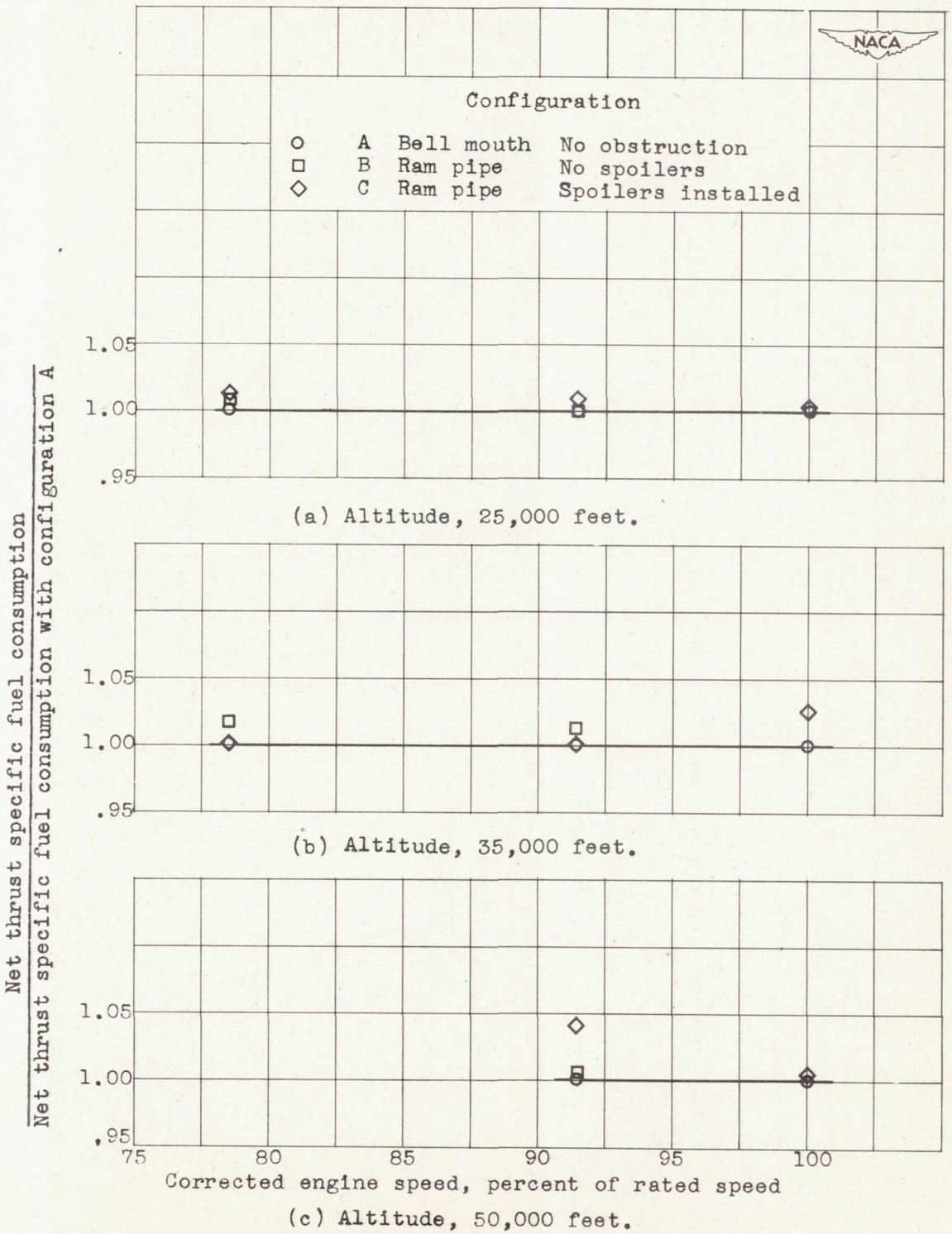

Figure 16. - Effect of engine-inlet-air velocity distribution on net thrust specific fuel consumption of first engine.

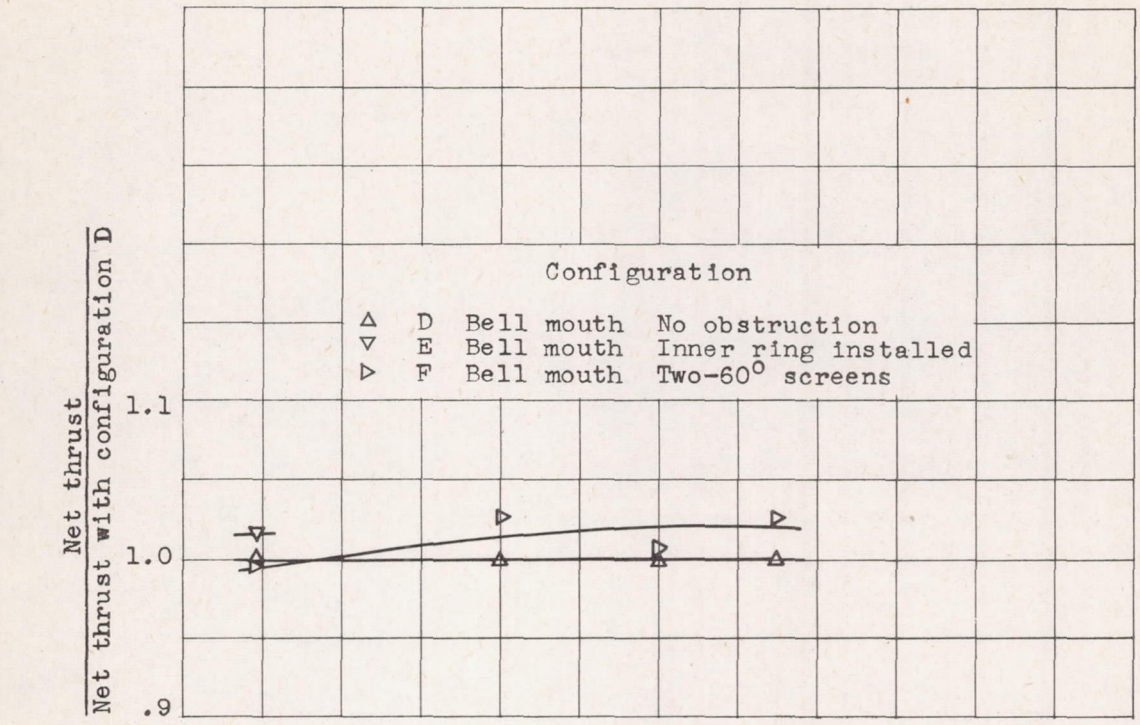

(a) Net thrust.

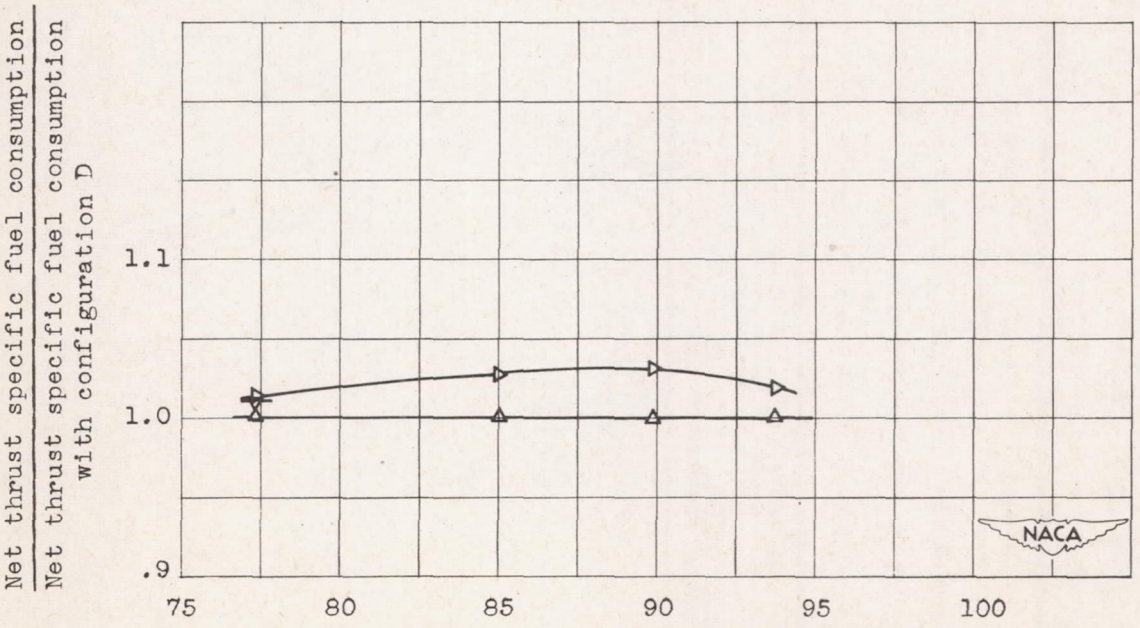

(b) Specific fuel consumption.

Figure 17. - Effect of engine-inlet-air velocity distribution on net thrust and specific fuel consumption of second engine. Altitude, 30,000 feet.